4-2024

MOLECULAR GEOMETRY CHANGES IN SOME CARBONYLS AND AROMATIC RINGS UPON ELECTRONIC EXCITATION: HERZBERG-TELLER VIBRONIC COUPLING AND UNITARY DUSCHINSKY ROTATION

Maryam Yahya Al-Sakkaf

MOLECULAR GEOMETRY CHANGES IN SOME CARBONYLS AND AROMATIC RINGS UPON ELECTRONIC EXCITATION: HERZBERG-TELLER VIBRONIC COUPLING AND UNITARY DUSCHINSKY ROTATION

Maryam Yahya Mohammed Al-Sakkaf

United Arab Emirates University

College of Science

Department of Chemistry

MOLECULAR GEOMETRY CHANGES IN SOME CARBONYLS
AND AROMATIC RINGS UPON ELECTRONIC EXCITATION:
HERZBERG-TELLER VIBRONIC COUPLING AND UNITARY
DUSCHINSKY ROTATION

Maryam Yahya Mohammed Al-Sakkaf

This thesis is submitted in partial fulfilment of the requirements for the degree of Master
of Science in Chemistry

April 2024

Cover: Duschinsky Matrix of CH_3COCH_3

(Photo: By Maryam Yahya Mohammed Al-Sakkaf)

Declaration of Original Work

I, Maryam Yahya Mohammed Al-Sakkaf, the undersigned, a graduate student at the United Arab Emirates University (UAEU), and the author of this thesis entitled *"Molecular Geometry Changes in Some Carbonyls and Aromatic Rings upon Electronic Excitation: Herzberg-Teller Vibronic Coupling and Unitary Duschinsky Rotation"*, hereby, solemnly declare that this is the original research work done by me under the supervision of Prof. Mohammed Toutounji, in the College of Science at UAEU. This work has not previously formed the basis for the award of any academic degree, diploma, or similar title at this or any other university. Any materials borrowed from other sources (whether published or unpublished) and relied upon or included in my thesis have been properly cited and acknowledged by appropriate academic conventions. I further declare that there is no potential conflict of interest concerning the research, data collection, authorship, presentation, and/or publication of this thesis.

Student's Signature:

Date: 20/5/2024

Advisory Committee

1) Advisor: Mohamad Toutounji

Title: Professor

Department of Chemistry

College of Science

2) Co-advisor: Mohammed Meetani

Title: Professor

Department of Chemistry

College of Science

3) Co-advisor: Alejandro Paz

Title: Associate Professor

Department of Chemistry

College of Science

Approval of the Master Thesis

This Master Thesis is approved by the following Examining Committee Members:

1) Advisor: Mohamad Toutounji
   Title: Professor
   Department of Chemistry
   College of Science

   Signature: M. Toutounji   Date: 13/5/2024

2) Member: Abdelouahid Samadi
   Title: Assistant Professor
   Department of Chemistry
   College of Science

   Signature: [signature]   Date: 13/5/2024

3) Member (External Examiner): Sharmarke Mohamad
   Title: Professor
   Department of Chemistry
   Institution: Khalifa University, UAE

   Signature: [signature]   Date: 13/5/2024

This Master Thesis is accepted by:

Dean of the College of Science: Professor Maamar Benkraouda

Signature _____

Date 2/7/2024 _____

Dean of the College of Graduate Studies: Professor Ali Al-Marzouqi

Signature ___Ali Hassan_____

Date _____July 4, 2024___

Abstract

The common assumption in probing the dynamical motion of molecules is that the molecular electronic activity depends weakly on vibrational coordinates on electronic excitation. Therefore, electron-vibration interaction, which is known as Vibronic Coupling (VC), may be ignored. The Herzberg-Teller theory of Vibronic Coupling (HTVC) is a breakdown of the Born-Oppenheimer Approximation (BOA) since nuclear and electronic degrees of freedom can no longer be separated. The inclusion of a single quantum of a non-totally symmetric vibrational mode changes the overall symmetry of the state and permits the transition. Often, this assumption may be invalid, especially in carbonyl and aromatic compounds. This thesis will use both quantum mechanics and electronic structure theory of molecules to probe the breakdown of this assumption in carbonyls (formaldehyde H_2CO, acetaldehyde CH_3CHO, and acetone CH_3COCH_3) and aromatic carbonyl compounds (benzaldehyde C_6H_5CHO and benzophenone $C_6H_5COC_6H_5$). This work will investigate the extent to which HTVC is significant by looking at nuclear coordinates deformation and electronic density redistribution upon electronic excitation. Non-totally symmetric vibrations are important to identify the coupled electronic states whereby intensity is borrowed from nearby electronic states in case of forbidden electronic transitions by symmetry in the FC region. This electronic density redistribution distortion may be due to the Duschinsky Matrix (DM) and HTVC interaction renders information on how the transition moment varies as the molecular geometry changes, giving rise to the non-Condon regime. This coupling should be probed to see if it is caused by orbital interaction and this interaction would give rise to non-adiabatic coupling. This molecular geometry alteration is so important for probing and hence understanding vibration-electron coupling in polyatomic molecules.

Keywords: Born Oppenheimer, Vibronic coupling, Duschinsky rotation and molecular, Herzberg-Teller effect and molecular geometry.

دراسة تغيرات الهندسة الجزيئية في بعض المركبات الكربونيلية والحلقية الأروماتية تحت تأثير الاستثارة الاكترونية متضمنة كلا من الاقتران الالكتروني الاهتزازي ل هيرزبيرغ-تيلر HTVC و تأثير دورانية داشينسكي DM

الملخص

الافتراض المشترك في استكشاف الحركة الديناميكية للجزيئات هو أن النشاط الإلكتروني للجزيء يعتمد بشكل ضعيف على الإحداثيات الاهتزازية عند الانتقال الإلكتروني. لذلك، يمكن تجاهل تفاعل الإلكترونات مع الاهتزازات (الانقطاع الاهتزازي). نظرية هيرزبيرغ-تيلر للاقتران الاهتزازي الاكترونـي هي انهيار لتقريب بورن-أوبنهايمر، حيث لا يمكن بعد الآن فصل درجات حرية النووية والإلكترونية. يؤدي إدراج كمية واحدة من وضع اهتزازي غير تمام التناظر إلى تغيير تمامي للحالة ويسمح بالانتقال. في كثير من الأحيان، يمكن أن يكون هذا الافتراض غير صحيح، خاصة في المركبات الكربونيلية والحلقات العطرية. سيستخدم هذا الأطروحة كل من ميكانيكا الكم ونظرية هيكل الكتروني للجزيئات لاستكشاف انهيار هذا الافتراض في الكربونيل (الفورمالدهيد، الأستيلدهيد، والأسيتون، والبنزالدهيد) والحلقات العطرية (البنزين، النفثالين، الأنثراسين). سيقوم هذا العمل بفحص مدى أهمية اقتران هيرزبيرغ-تيلر للاهتزازات من خلال النظر إلى تشوه إحداثيات النوى وإعادة توزيع الكثافة الإلكترونية عند الانتقال الإلكتروني. الاهتزازات غير التمامية التناظرية مهمة لتحديد الحالات الإلكترونية المقترنة حيث يتم استعارة الشدة من الحالات الإلكترونية القريبة في حالات الانتقال الإلكتروني المحظورة من الناحية التناظرية في منطقة فرانك-كوندون. يمكن أن يكون هذا التشوه في إعادة توزيع الكثافة الإلكترونية ناتجًا عن دورانية داشينسكي والاقتران هيرزبير-غ-تيلر. يقدم التفاعل هيرزبيرغ-تيلر معلومات حول كيفية تغير لحظة الانتقال مع تغير هندسة الجزيء، مما يؤدي إلى الانتقال إلى نطاق غير كوندون. ستستخدم هذه الرسالة كل من ميكانيكا الكم ونظرية هيكل الكتروني للجزيئات لاستكشاف انهيار هذا الافتراض في المركبات الكربونيل (الفورمالدهيد، الأستيلدهيد، والأسيتون) والحلقات العطرية (البنزالدهيد والبنزوفينون). سيقوم هذا العمل بفحص مدى أهمية اقتران هيرزبيرغ-تيلر للاهتزازات من خلال النظر إلى تشوه إحداثيات النوى وإعادة توزيع الكثافة الإلكترونية عند الانتقال الإلكتروني. الاهتزازات غير التمامية التناظرية مهمة لتحديد الحالات الإلكترونية المقترنة حيث يتم استعارة الشدة من الحالات الإلكترونية القريبة في حالات الانتقال الإلكتروني المحظورة من الناحية التناظرية في منطقة فرانك-كوندون. يمكن أن يكون هذا التشوه في إعادة توزيع الكثافة الإلكترونية ناتجًا عن دورانية داشينسكي والاقتران هيرزبيرغ-تيلر. يقدم التفاعل هيرتسبرغ-تيلر معلومات حول كيفية تغير لحظة الانتقال مع تغير هندسة الجزيء، مما يؤدي إلى الانتقال إلى نطاق غير كوندون. يجب فحص هذا الاقتران لرؤية ما إذا كان ما يسببه تفاعل الأوربيتالات وما إذا كان هذا التفاعل سيؤدي إلى اقتران غير آدمي. هذا التغيير في هندسة الجزيء مهم لاستكشاف وبالتالي فهم اقتران الاهتزاز بالإلكترون في الجزيئات متعددة الذرات.

مفاهيم البحث الرئيسية: تقريب بورن-أوبنهايمر، الاقتران الاهتزازي الكتروني، دورانية داشينسكي، تأثير هيرزبيرغ-تيلر وهندسة الجزيء.

Acknowledgments

My deepest gratitude goes to my advisor, Prof. Mohamad Toutounji, for his unwavering guidance, expertise, efforts, motivation, and endless patience during my master's journey. Undoubtedly, it has been an honor and pleasure working with him, and I look forward to future collaboration.

I would also like to express my gratitude to my co-advisors, Dr. Alejander Perez and Prof. Mohammed Meetani, for their valuable insights and contributions. Their support has been instrumental in the successful completion of this research.

I will forever be thankful to the Master program coordinator in the Department of Chemistry, Prof. Yaser Greish for his enlightening suggestions, useful discussions, and continuous help.

I am also thankful to all the members of the Department of Chemistry for their support and guidance through my graduate studies, and to all my lovely friends and colleagues for their encouragement and support.

I express my acknowledgment to all the members of the College of Science and the College of Graduate Studies at the United Arab Emirates University for their support and guidance through my graduate studies.

Finally, special thanks go to my family, for their everlasting hope, care, and concern to relieve my worries and stress.

Dedication

To my beloved parents, sisters, brothers, and my little family.

Table of Contents

List of Tables

List of Figures

List of Abbreviation

BO	Born Oppenheimer
BOA	Born-Oppenheimer Approximation
DE	Duschinsky Rotation, Duschinsky Effect
DM	Duschinsky Matrix
FC	Franck-Condon
HOMO	Highest Occupied Molecular Orbitals
HT	Herzberg-Teller
HTVC	Herzberg-Teller Vibronic Coupling
LUMO	Lowest Unoccupied Molecular Orbitals
MO	Molecular Orbital
NA	Non-Adiabatic
NAC	Non-Adiabatic Coupling
TDDFT	Time-Dependent Density Functional Theory
VC	Vibronic Coupling

Chapter 1: Introduction

1.1 Overview

1.1.1 Overview of the Born-Oppenheimer Approximation and its Role in Separating Nuclear and Electronic Degrees of Freedom

Born Oppenheimer Approximation (BOA) is a fundamental concept in molecular physics that allows for the separation of nuclear and electronic motion in molecules [1]. This approximation is based on the observation that the nuclei in a molecule are much more massive than the electrons, resulting in the nuclei moving much more slowly compared to the rapid motion of the electrons [2]. Therefore, the electrons can adjust rapidly to changes in the nuclear configuration, allowing the electronic wavefunction to be treated independently of the nuclear coordinates [3]. This separation simplifies the mathematical treatment of the electronic structure problem by reducing the complexity of solving the Schrödinger equation [3]. By neglecting the nuclear kinetic energy in the Hamiltonian, the BOA allows the determination of the electronic energy levels and wavefunctions of molecules [3]. In this approximation, electronic wavefunction explicitly depends on the electronic coordinates, representing the positions of the electrons, while being parametrically dependent on the nuclear coordinates, representing the positions of the nuclei. This separation enables the electronic motion to be treated separately from the nuclear motion. The electronic wavefunction adjusts instantaneously to changes in the nuclear coordinates, resulting in an equilibrium state between the electronic and nuclear motions. This approximation plays a crucial role in understanding the electronic structure of molecules. By treating the electronic and nuclear degrees of freedom independently, it becomes possible to calculate the electronic energy levels and wavefunctions for each value of the nuclear position parameter. This approximation is highly effective and accurate for describing the electronic structure and properties of most molecules. It has been extensively validated by its successful application to a wide range of molecular systems. The separation of nuclear and electronic motion simplifies the theoretical treatment of the electronic structure problem, enabling the calculation of important molecular properties such as electronic energies, wavefunctions, and spectroscopic transitions. The BOA has been proven to be a powerful tool in understanding the electronic

structure and properties of molecules, providing valuable insights into chemical bonding, reactivity, and spectroscopy. However, it is important to note that BOA has limitations. In situations where the coupling between electronic and vibrational degrees of freedom becomes significant, such as in systems with strong vibronic coupling, the approximation breaks down [4].

1.1.2 Limitations of the Born-Oppenheimer Approximation and its Breakdown in the Presence of Vibronic Coupling

This approximation provides a powerful framework for understanding the electronic structure of molecules by separating the nuclear and electronic degrees of freedom. However, it has inherent limitations that become particularly relevant in systems with strong vibronic coupling, where the interaction between the electronic and vibrational motion plays a significant role. The Franck-Condon (FC) principle is a fundamental concept in molecular spectroscopy that describes how electronic transitions occur in molecules. It states that the most likely electronic transitions are those in which the nuclei do not change their positions [1, 2]. This is because electronic transitions happen much faster than nuclear motion. The FC factors are mathematical entities that quantify the probability of an electronic transition between two vibrational states [1, 2]. They are important for understanding the vibrational structure of electronic spectra and for designing lasers that emit light at specific wavelengths. One of the key limitations of the FC principle is that it does not account for vibronic coupling [3]. Vibronic coupling is the interaction between electronic and vibrational degrees of freedom in molecules. It can modify the energy levels of electronic states, the transition probabilities between electronic states, and the selection rules governing electronic transitions.

Vibronic coupling is particularly important in carbonyl compounds and aromatic rings [3]. These compounds exhibit characteristic electronic transitions associated with the excitation or de-excitation of the π electrons. Vibronic coupling can alter the energy levels of these electronic states, the transition probabilities between electronic states, and the selection rules governing electronic transitions. This can lead to changes in the absorption and emission spectra, the color and optical properties, and the reactivity of these compounds.

2

1.1.3 The Concept of the Franck-Condon Principle

The FC principle assumes that the nuclei do not change their positions during an electronic transition [1, 2] This is because electronic transitions happen much faster than nuclear motion. As a result, the most likely electronic transitions are those in which the initial and final vibrational states of the nuclei are the same. FC factors are calculated by integrating the vibrational wavefunctions of the initial and final states [1, 2]. The larger the overlap between the two wavefunctions, the more likely the transition is to occur. The FC principle can be used to explain the vibrational structure of electronic spectra [1, 2]. For example, the absorption spectrum of a molecule will show a series of peaks, each corresponding to a different vibrational transition. The intensity of each peak is determined by the FC factor for that transition.

1.1.4 The Concept of Vibronic Coupling

The Vibronic Coupling (VC) is the interaction between electronic and vibrational degrees of freedom in molecules [3]. It can arise from several factors, such as the presence of strong electric fields or the coupling of electronic and vibrational transitions. This concept can modify the energy levels of electronic states, the transition probabilities between electronic states, and the selection rules governing electronic transitions [1, 3]. For example, vibronic coupling can allow electronic transitions that are forbidden by symmetry rules to occur. Vibronic coupling is particularly important in carbonyl compounds and aromatic rings [1, 3]. These compounds exhibit characteristic electronic transitions associated with the excitation or de-excitation of the π electrons. Vibronic coupling can alter the energy levels of these electronic states, the transition probabilities between electronic states, and the selection rules governing electronic transitions. This can lead to changes in the absorption and emission spectra, the color and optical properties, and the reactivity of these compounds.

One example of VC is the Kasha rule [1]. The Kasha rule states that the lowest energy electronic state of a molecule is the most fluorescent state. This is because the vibrational relaxation of the molecule after electronic excitation is much faster than the fluorescence process. As a result, the molecule is most likely to fluoresce from the lowest energy vibrational state of the lowest energy electronic state. The FC principle stands as a

fundamental concept, shaping our understanding of electronic transitions [4]. Rooted in quantum mechanics, this principle illuminates the likelihood of electronic transitions occurring without simultaneous nuclear movement. Central to this principle are the FC factors, mathematical entities that quantify the probability of such transitions [5]. In this exploration, we delve into the depths of the FC principle, unraveling its theoretical underpinnings and unveiling the pivotal role played by FC factors in molecular spectroscopy. Vibronic transitions are simultaneous changes in the electronic and vibrational energy levels of a molecule [1]. When an electronic transition occurs, the nuclei in the molecule are subjected to a change in Coulombic force due to the redistribution of electronic charge. This means that the molecular potential energy surface, which governs the motion of the nuclei, changes. In response, the nuclei vibrate more vigorously, and the absorption spectrum shows a structure that is characteristic of the vibrational energy levels of the molecule.

1.2 Research Objectives

The Herzberg-Teller Vibronic Coupling (HTVC) and the Duschinsky Matrix (DM) are two important ideas in vibronic spectroscopy. HTVC connects the electronic and vibrational parts of molecules, causing the vibronic bands in molecular spectra to separate. Meanwhile, the DM explains how the vibrational frequencies and strengths change because of HTVC. This project aims to demonstrate the theoretical nature of electronic spectra incorporating the effects of the DM and HTVC using software, primarily Gaussian. We will investigate the evolution of nuclear geometry and subsequent changes in symmetry, clarifying how these transformations lead to a new point group for the molecule in its excited state over time. This scenario violates the FC principle due to the distortion in molecular symmetry (point group), resulting in the initial state differing from the final electronic state. Addressing this, both DM and HTVC must be considered. achieve this, we will focus on the carbonyl structure and its potential enhancement of vibronic coupling. Our primary compounds of interest encompass simple carbonyls: 1- Formaldehyde: CH_2O 2- acetaldehyde:CH_3CHO 3- acetone CH_3COCH_3 4- benzaldehyde: C_6H_5CHO and 5- benzophenone: $C_6H_5COC_6H_5$. Furthermore, this research aims to examine the application

of DM specifically in the first four compounds and will compare those effects with the corresponding Non-Adiabatic Coupling (NAC) values.

1.3 Relevant Literature

The BOA simplifies the Schrödinger equation for molecules by assuming that the electrons move much faster than the nuclei. This allows us to treat the electrons as if they were stationary, while the nuclei move more slowly. The electronic wavefunction depends on the nuclear positions, but it can instantly adjust to keep up with the nuclear motion. This is known as the adiabatic approximation. The nuclear wavefunction, on the other hand, depends on the electronic wavefunction, but not explicitly on the nuclear positions. This is because the nuclei only see the averaged electron distribution. The BOA leads to a Potential Energy Surface (PES) for the nuclei in each electronic state. The PES is different for each electronic state because the interaction of the nuclei with the averaged electron distribution is different for each state. This approximation breaks down when the kinetic energy terms for the nuclear motion become comparable to the electronic terms. This can happen in certain cases, such as when the molecule is excited to a high-energy electronic state. However, the BOA is usually a good approximation and is an important tool in molecular spectroscopy and energy transfer.

In simpler terms, BOA allows us to treat the electrons and nuclei in a molecule as if they were moving on separate tracks. The electrons move much faster than the nuclei, so they can instantly adjust to keep up with the nuclear motion. This allows us to calculate the electronic energy levels and wavefunctions for the molecule without having to worry about the nuclear motion. The nuclear motion, on the other hand, depends on the averaged electron distribution. This averaged electron distribution creates a potential energy surface for the nuclei, which is different for each electronic state. It allows us to understand how molecules absorb and emit light, and how they transfer energy between different vibrational states.

Intensity borrowing or stealing is a process by which a transition that is normally forbidden can become allowed by borrowing intensity from a nearby allowed transition. This can happen when two electronic states are coupled strongly.

Group theory can be used to predict which transitions are allowed and which are forbidden, and it can also be used to calculate the amount of intensity borrowing that occurs. This information can be used to understand and interpret electronic spectra.

1.4 Herzberg-Teller Concept

The Herzberg-Teller (HT) principle explains the vibronic coupling in the molecular electronic spectra. It describes the coupling between electronic and nuclear motions in a molecule during a spectroscopic transition. According to this concept, the intensity of a vibrational transition in the electronic spectrum (like electronic absorption or emission) can be influenced by the vibrational modes that change during the electronic transition and how these changes affect the intensity of the electronic spectrum.

1.5 Intensity Borrowing

Intensity borrowing occurs when vibrational transitions that are nominally forbidden become allowed due to vibrational-electronic (vibronic) coupling. These transitions are termed "borrowed" because they gain intensity from the electronic transition, even though they would typically be weak or forbidden based solely on selection rules for vibrational transitions.

1.6 Relation between Intensity Borrowing and Herzberg-Teller Concept

The HT concept explains intensity borrowing by illustrating how certain vibrational modes can couple with the electronic transition, causing changes in the selection rules and thus allowing normally forbidden vibrational transitions to become observable.

When a molecular electronic transition occurs, it induces changes in the molecular potential energy surfaces. These changes can lead to modifications in the vibrational wavefunctions and their overlap between initial and final states. Vibrational modes that do not change during the electronic transition (i.e., those exhibiting vibrational progressions parallel to the excited electronic state) can interact with this electronic transition through vibronic coupling, resulting in borrowed intensity.

In essence, the HT concept provides the theoretical framework to understand how vibronic coupling influences the intensity of vibrational transitions in electronic spectra. It helps

elucidate why certain vibrational transitions, which would normally be forbidden based on purely vibrational selection rules, become allowed or exhibit increased intensity due to their interaction with the electronic transition.

Therefore, intensity borrowing can be conceptually related to the HT concept by highlighting how vibronic coupling influences the selection rules governing the intensity of vibrational transitions in molecular electronic spectra.

Here is an example of how intensity borrowing can occur:

1.7 Illustrative Example

Consider a molecule that has two electronic states, the ground state, and an excited state. The excited state is coupled strongly with a third state, which is also an excited state. The third state is allowed to decay to the ground state, but the excited state is nominally forbidden to decay to the ground state. However, because the excited state is coupled strongly to the third state, the excited state can borrow intensity from the third state and decay to the ground state. This is called intensity borrowing or stealing. Intensity borrowing can be used to explain several phenomena in electronic spectroscopy, such as the appearance of weak transitions in spectra that are normally forbidden. It can also be used to study the coupling between electronic states. Molecular geometry may change upon electronic excitation, in response to the exerting molecular forces, causing the dipole moment to decrease or increase. (For example, upon electronic excitation, water molecular geometry changes considerably, resulting in a dipole moment shift from 1.85 D to 0.0 D by going from bent (ground state) to linear (excited state), and CH_2O geometry Changes from trigonal planar to a pyramidal configuration (excited state), thereby shifting its dipole moment from 2.33 D to 1.6 D in the singlet state, vide infra for more details. This change in dipole moment is ascribed to the relevant geometry change, and therefore point group symmetry changes, upon electronic excitation/emission. This alteration of geometry modifies the nuclear coordinates and, therefore, how the corresponding Molecular Orbitals (MOs) depends on these coordinates. The change in the electronic dipole moment is ascribed to coherence between the ground and excited states, thereby setting up the transition dipole moment of the molecule. As such, the transition dipole moment dynamics

is an essential part of understanding spectroscopy, particularly HT coupling. Thus, excited molecular spectroscopy may readily capture the corresponding geometry change.

While rigid molecules experience negligible molecular distortion upon electronic excitation, [20] some molecules exhibit noticeable distortion, due to electron density redistribution and molecular re-equilibration; hence adopting a different point group. Others show strong deformation, which will not be discussed herein. While molecular geometry change implies a change of bond length (linear displacement) and strength (force constant), molecular distortion may very well involve HTVC and DM of normal modes upon electronic excitation [20-27].

Because rigid molecules experience no symmetry change, and thus retain their ground state molecular geometry (nuclear coordinates), upon electronic excitation, they can be designated as FC molecules. Both DM and HTVC contribute insignificantly to FC molecules on excitation. On the other hand, non-rigid molecules allow the vibrations to interact appreciably with the electronic state, thereby leading to nuclear coordinates rearrangement, or point group change, evoked by HTVC and DM [21]. As such, vibronic coupling that caused by HTVC and DM leads to the evolution of the nuclear coordinates upon electronic excitation as time elapses. The difference in nuclear configuration between the initial and final electronic states is normally accompanied by electron density redistribution and hence different electronic configurations. Anthracene is an example of rigid molecules [27]. normally do not result in a molecular point group change upon excitation, thereby retaining their symmetry, hence no distortion.

Chapter 2: Theoretical Background

2.1 Mathematical Representation of the Franck-Condon Principle

At its core, the FC principle posits that electronic transitions between molecular states occur instantaneously, without any nuclear motion. This phenomenon is especially pertinent during the absorption or emission of light, where electronic states change, but the nuclear configuration remains fixed. Mathematically [10], this principle is expressed as:

$$| < \Psi_f(R) | \Psi_i(R) > |^2 \propto (E_f - E_i) \tag{1}$$

Where $\Psi_f(R)$ and $\Psi_i(R)$ represent the final and initial nuclear wave functions, R denotes nuclear coordinates, and E_f and E_i are the final and initial electronic energies, respectively.

FC factors, denoted as P(Δv), quantify the transition probability between vibrational states Δv of different electronic states. These factors are pivotal in understanding the intensity distribution of spectral bands. The FC factor for a transition involving a change of v vibrational quanta is given by the overlap integral:

$$P(\Delta v) = | \int \Psi_v^f(R)\Psi_v^i(R)dR |^2 \tag{2}$$

Here, $\Psi_v^f(R)$ and $\Psi_v^i(R)$ represent the final vibrational state and initial vibrational ground state wave functions, respectively.

2.2 Vibronic Structure

Vibronic transitions are transitions between different vibrational levels of different electronic states. These transitions are important because they can provide information about the potential energy surfaces of different electronic states. Such transition is represented as:

$$\Psi_{elec,i}\Psi_{vib,iI} \rightarrow \Psi_{elec,f}\Psi_{vib,fF}$$

Where electronic and vibrational wavefunctions are categorized based on both their electronic state (i or f) and the quantum state of the vibrational oscillator (I or F) because

the potential energy surfaces vary for different electronic states, leading to distinct vibrational wavefunctions. [10]

For clarification:

Ψ_i:is the electronic wavefunction of electronic state i

Ψ_f: is the electronic wavefunction of electronic state f

Now:

Ψ_{iI} : is the vibrational wavefunction for the quantum vibrational state I within the that electronic state, i.

Ψ_{fF} : is the vibrational wavefunction for the quantum vibrational state F within the that electronics state, f.

For a transition: i and I denote initial conditions, while f and F denote final conditions.

The probabilities of these transitions can be calculated using the Taylor series expansion

$$< \Psi_{elec,f} \Psi_{vib,fF} \,|\, \mu_z \,|\, \Psi_{elec,i} \Psi_{vib,iI} > =$$

$$\int dR \Psi *_{vib,fF} (R) \left\{ \mu_{if}, z(R_0) + \Sigma_j \left(\frac{\partial \mu_{if},z}{\partial R_j} \right) (R_j - R_{j0}) + \cdots \right\} \Psi_{vib,iI} (R) \qquad (4)$$

of the electronic dipole moment matrix element equation:

Where: μ_z is the electronic dipole moment operator along the z direction, and R is the vibrational coordinate. The presence of " j " in the equation denotes different terms in the Taylor series expansion of the electronic dipole moment matrix element with respect to the nuclear coordinates (R). Each " j " would correspond to a specific term in the expansion, enabling a more detailed description of how the electronic dipole moment varies concerning the nuclear geometry. Please note that the electronic matrix element differs from a permanent dipole moment (which is the expected value of μ in the electronic state Ψ_i). Instead, it represents a transition dipole moment, which is the matrix element of μ between two distinct electronic states.

This expansion is useful because it can consider the changes in the electronic dipole moment due to the vibration of the nuclei. This series expansion of the electronic dipole

moment matrix element is a powerful tool to understand and calculate the probabilities of vibronic transitions in a variety of molecular systems. For example, it can be used to study the absorption and emission of light, the reactions of molecules, and the transport of energy in molecules. The electronic matrix element here is the transition dipole moment between the two electronic states. This is not the same as the permanent dipole moment of a molecule. The transition dipole moment can be nonzero even in a completely nonpolar molecule. The vibrational coordinate is a measure of the displacement of the nuclei from their equilibrium positions. It is a useful quantity for describing vibrational transitions.

Referring to Equation 4, and under the Condon approximation, the integral known as the vibrational overlap integral, denoted as $\mu_{if}^z(R_0)$ determine the strength of an electronic transition as:

$$\mu_{if}^z(R_0) = \int dR \Psi_{vib,fF}^*(R)\Psi_{vib,iI}(R) \tag{5}$$

In the context of a vibrational infrared transition where $\Psi_{vib,fF}$ and $\Psi_{vib,iI}$ represent vibrational levels within the same electronic state, the integral would equate to zero unless I=F. However, in this scenario, $\Psi_{vib,iI}$ represents a vibrational eigenstate of the potential energy surface for the ground electronic state, $\phi(R)$, while $\Psi_{vib,fF}$ characterizes an eigenstate of a distinct potential energy surface for the excited electronic state, $\phi'(R)$. In general, differences exist in both the equilibrium internuclear separation and curvature between these surfaces, causing eigenstates characterized by distinct quantum numbers to be non-orthogonal, Hence, there's no inherent reason for the $\mu_{if}(R_0)$ term to be zero. The term in $\mu_{if}(R_0)$ is usually considerably larger than the one involving the derivatives, $\partial \mu_{if}^z/\partial R_j$.

The integral over vibrational coordinates, as denoted in Equation 5, is termed the "vibrational overlap integral." The probability of the transition relies on the square of the matrix element, $|\mu_{if}^z(R_0)|^2 \, |\int dR \Psi_{vib,fF}^*(R)\Psi_{vib,iI}(R)|^2$. The second factor, the square of the vibrational overlap integral, is termed the "Franck–Condon factor." This factor determines the relative strengths of various vibrational sublevels within a given electronic transition. The overall intensity of the transition is determined by the electronic component, $|\mu_{if}^z(R_0)|^2$.

The Franck–Condon factors follow a vibrational sum rule, where the sum across all Franck–Condon factors originating from a particular initial vibrational state is considered.

$$\sum_F \big| < \Psi_{vib,fF} \Psi_{vib,iI} > \big|^2 =$$

$$\sum_F < \Psi_{vib,fF} \Psi_{vib,iI} >< \Psi_{vib,fF} \Psi_{vib,iI} > = <\Psi_{vib,iI} \Psi_{vib,iI} > = 1 \qquad (6)$$

Before we go any further, we need to take a closer look at the nature of the vibrational wave function for a polyatomic molecule. In the harmonic oscillator approximation, the vibrational wavefunctions can be broken down into products of wavefunctions for each of the individual normal modes, like this:

$$\Psi_{vib}^{total}(R) = \Psi_{v1}(R_1)\Psi_{v2}(R_2)\Psi_{v3}(R_3) \dots . \Psi_{vn}(R_n) \qquad (7)$$

This means that the 3N−6-dimensional vibrational wavefunctions in Equation 5 can be broken down into a product of one-dimensional wavefunctions. In other words, the vibrational wavefunction of a molecule can be thought of as a product of the vibrational wavefunctions of each of its normal modes. This is a very useful simplification because it allows us to treat each normal mode independently. This assumes that the normal modes of the ground and excited electronic states are the same, which may not be the case. In general, the normal modes of the excited state are linear combinations of the normal modes of the ground state. This introduces what is known as the Duschinsky Effect (DE) or Duschinsky Matrix (DM) [2]. In the context of Equation 4, the subsequent term in the expansion of the electronic transition moment, delves into potential energy surfaces and vibrational wavefunctions associated with a non-totally symmetric vibrational coordinate. When atoms shift in the positive or negative directions, creating structures that are indistinguishable and possess identical energy, the potential surfaces must be even functions of the coordinate. Consequently, the vibrational wavefunctions exhibit symmetry: they are either all even (for even vibrational quantum numbers, v) or all odd (for odd v). Considering the $\sum_j (\partial \mu_{if}^z / \partial R_j) R_j$ term, where the summation encompasses all normal modes R_j with the definition R=0 at the equilibrium geometry, the matrix element can be expressed as:

$$\mu_{if}^z = \sum_j \left(\frac{\partial \mu_{if}^z}{\partial R_j} \right)_0 \int dR \Psi_{vib,fF}^*(R) R_i \Psi_{vib,iI}(R) \qquad (8)$$

When $\mu_{if}(R_0)$ is non-zero, its derivatives $(\partial\mu_{if}/\partial R_j)_0$ are typically much smaller, making these "non-Condon" terms perturbation minorly on the electronic spectrum. However, if $\mu_{if}(R_0)$ is zero due to the symmetry of electronic wavefunctions, the situation becomes more intriguing. In linear molecules, altering bond lengths doesn't affect the point group. Consequently, $\mu_{if}(R_0)$ and $(\partial\mu_{if}/\partial R)$ share the same symmetry. Higher terms in the transition moment's series expansion don't alter the symmetry selection rules; they only influence the electronic transition moment's magnitude due to the electronic wavefunction's dependence on internuclear separation. For linear molecules comprising three or more atoms falling under $D_{\infty h}$ or $C_{\infty v}$ symmetry, non-Condon terms $(\partial\mu_{if}/\partial R_j)_0$ can be non-zero even when $\mu_{if}(R_0)$ is zero, provided represents a non-totally symmetric vibrational coordinate. This phenomenon occurs because shifting nuclei along such a coordinate alters the molecule's point group, enabling transitions that were previously disallowed. The term $(\partial\mu_{if}/\partial R_j)_0$ can lead to an electric dipole-allowed transition if the product of the electronic initial state Ψ_i, the electronic final state, Ψ_i, the dipole operator μ, and the vibrational coordinate either is or contains the symmetric representation.

2.3 Illustrative Example

For the orbitally forbidden transition between the ground state (X $^1A_1$) and the first excited state ($\tilde{A}^1A_2$) in CH_2O, it is forbidden because the two electronic states have different symmetries. However, the transition can become allowed if it is coupled to a B_2 vibration. The B_2 vibration has the same symmetry as the product of the X $^1A_1$ and $\tilde{A}$ $^1A_2$ electronic states, so the vibronic transition B_2 $\tilde{A}$ $^1A_2$ is electric dipole allowed. The NAC vector between the X $^1A_1$ and $\tilde{A}$ $^1A_2$ electronic states is responsible for the coupling of the two states to the B_2 vibration. This coupling gives rise to the vibronically allowed transition B_2 $\tilde{A}$ $^1A_2$. The NAC vector and VC can also be used to describe the effects of vibronic coupling on the rate of non-adiabatic transitions. When the VC is strong, the wavefunctions of the electronic states can mix, and this can make it easier for the electrons to tunnel from one state to the other. This can lead to an increase in the rate of non-adiabatic transitions.

2.4 Nonadiabatic Coupling

Conical intersection, intersystem crossing and internal conversion are main examples of the phenomenon NAC. When Conical intersections are degeneracies, they facilitate NAC between excited states. As an example: both intersystem crossing and internal conversion break down BOA. Again, In this scenario, lower case ('i', 'f') denote distinct electronic states $\Psi_i \; and \; \Psi_f$, while upper case ('I', 'F') represent vibrational states $\Psi_I \; and \; \Psi_F$. , and let represent the their vibronic matrix Hamiltonian as :

$$H = \begin{pmatrix} H_{ii}(R) & H_{if}(R) \\ H_{fi}^{*}(R) & H_{ff}(R) \end{pmatrix} \tag{9}$$

in the basis of those two electronic states, $\Psi_i \; and \; \Psi_f$, with R be the nuclear coordinate and other (non-vibrational) degrees o freedom are integrated outside our assumption. Now, by definition, and at some R, these states are considered as Born Oppenheimer (BO) states if they diagonalize H at that selected R, and here two conditions are needed as below:

1) $H_{ii}(R) = H_{ff}(R)$,

2) $H_{if}(R) = 0$.

There are 3N-6 degrees of freedom. (assuming nonlinear molecule), where N here is the number of atoms of that molecule). Now let us divide them:

[3N-6-2] are internal nuclear degrees of freedom composing what is called the seam subspace and those are degenerate along that subspace. The remaining two. The other two remaining degrees of freedom, known as the branching space, lose their degeneracy by infinitesimal displacement generating what we mentioned above, a conical intersection. And as the name suggests, if that was plotted in 3D, it seems like a double cone at the intersection point. Let us focus on the branching space:

With two states (degrees of freedom), here the branching space is a span of a pair of two vectors: let us denote them as g_{if} and h_{if}.

g_{if} is the gradient vector of the two states as:

$$g_{if} = \frac{\partial E_i}{\partial R} - \frac{\partial E_f}{\partial R} \tag{10}$$

h_{if} here is the NAC vector:

$$h_{if} = \langle \Psi_i \left| \frac{\partial \mathbf{H}}{\partial R} \right| \Psi_f \rangle \tag{11}$$

Another considerable vector is the NAC one, d_{if}:

$$d_{if} = \langle \Psi_i \left| \frac{\partial}{\partial R} \right| \Psi_f \rangle = \frac{h_{if}}{Ef - Ei} \tag{12}$$

The VC is derived from the BOA. In this approximation, the electronic and nuclear motions are treated separately, while VC is the interaction between the electronic and nuclear motions. The NAC is the change in the electronic wavefunction due to a change in the nuclear coordinates. It can be expressed as a derivative of the electronic wave function with respect to the nuclear coordinates. The DM is a unitary transformation that diagonalizes the VC matrix. The nonadiabatic coupling matrix can be obtained from the DM and the electronic wavefunctions.

2.5 Duschinsky Effect

Under the vibronic approximation, the normal coordinates of two electronic states of the molecule can be linked through a linear transformation that rearranges and combines the ground state normal modes with the excited state normal modes. This transformation accounts for the differences in potential energy surfaces and nuclear displacements between the two states.

$$R_i = JR_f + k \tag{13}$$

This relationship, first formulated by Duschinsky, is now recognized as the Duschinsky transformation [11, 28]. In Equation (15), R_i denotes the coordinates of the normal modes of the initial state, while R_f represents the coordinates of the normal modes of the excited state. The matrix J symbolizes a rotation matrix, commonly referred to as the DM. It characterizes the blending or mixing of normal modes between the two states. k indicates potential energy surface displacements for both electronic states along the normal coordinates.

Chapter 3: Research Methods

3.1 Research Design and Theoretical Procedure

Our research questions include inquiries into whether there exists a correlation between coordinate deformation (alterations in molecular geometry) and non-rigid molecules, and if HTVC has a significant relationship with non-adiabatic coupling. Our research relies heavily on advanced electronic structure theory and sophisticated mathematical software tool: Gaussian. By utilizing these tools, we delve into the complexities of the Schrödinger equation within a many-body system. Our approach combines Time-Dependent Density Functional Theory (TDDFT) and ab initio techniques from many-body quantum theory. These methods provide the framework for examining the breakdown of the FC principle or BOA. We also analyze how the electronic transition dipole moment depends on the variations in nuclear positions within the molecules under study.

Our goal is to uncover the intricate relationships between HTVC and coordinate deformation in carbonyl compounds. Beginning with a fundamental molecule which is CH_2O, we aim to establish links between HTVC, coordinate deformation, and the specific molecular structure being investigated. As our research advances, we explore more complex molecules including both CH_3CHO and CH_3COCH_3 as two simple carbonyl compounds. Later we move to aromatic carbonyl compounds including C_6H_5CHO and $C_6H_5COC_6H_5$.

3.2 Data Collection

3.2.1 Simple Carbonyl Compound: CH_2O

In Tables 1, 4, 7, 10 and 13, the best light polarization data was determined by applying the symmetry rules taking into consideration the symmetry of normal modes. Those modes with symmetry labels that add to the total symmetry of the transition were tested to see what best light polarization will match the corresponding affecting transition dipole moment including those normal modes. Each point group has its own symmetry labels and direct product table, and for this we referred to Atkins's symmetry appendix [2]. Figure 1 reveals the CH_2O structure, while Figure 2 shows the vibronic spectrum of CH_2O.

Table 2 illustrates changes in positions due to non adiabatic coupling between state S_0 and S_1 in formaldehyde CH_2O. It illustrates atomic movements in CH_2O and their implications for NAC. A considerable displacement of one of the hydrogen atoms by 0.320896 Å along the Y-axis significantly influences NAC, potentially altering electron interactions between states (Table 3). Additionally, the opposing movements by the other hydrogen atom along the Y-axis may complicate NAC, impacting electron transitions within the molecule. No mentioned participation of the carbonyl group in NAC.
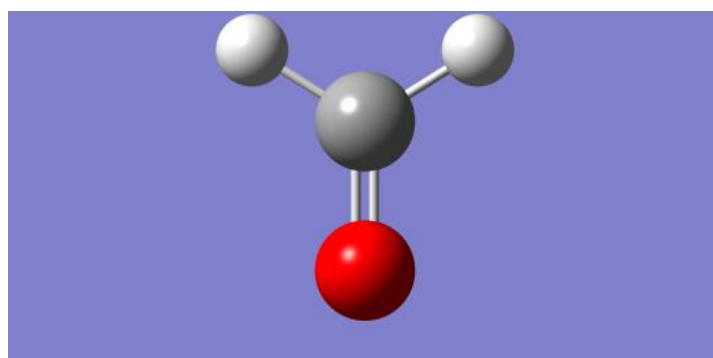
Figure 1: CH_2O Structure

Table 1: Symmetry and Polarization of CH_2O

Symmetry label	State/mode	Best light polarization
A_1	Ground state S_0	Z-polarized light
B_1	Excited state S_1	X-polarized light or y-polarized light
A_1	C=O stretching	Z-polarized light
B_1	C-H stretching	X-polarized light or y-polarized light
B_2	H-C-H bending	X-polarized light or y-polarized light

Table 2: Vibronic Transitions in CH_2O

Transition	Initial state →Final state	Transition energy (cm^{-1})	Oscillator strength	Wavelengths (nm)
1	$0 \rightarrow 0$	27148.8199	0.0003827	368.25
2	$0 \rightarrow 1^1$	27636.3048	0.0003886	361.65
3	$0 \rightarrow 1^2$	28123.7898	6.44 x10-05	355.06
4	$0 \rightarrow 3^1$	28420.1415	0.0006316	351.86
5	$0 \rightarrow 4^1$	28522.4415	0.0001477	351.20
6	$0 \rightarrow 3^1 1^1$	28907.6264	0.0006525	345.39
7	$0 \rightarrow 4^1 1^1$	29009.9265	0.0001465	344.86
8	$0 \rightarrow 3^1 1^2$	29395.1114	0.0001129	340.02
9	$0 \rightarrow 3^2$	29691.463	0.0004448	29691.463
10	$0 \rightarrow 4^1 3^1$	29793.7631	0.0002267	333.00
11	$0 \rightarrow 3^2 1^1$	30178.948	0.0004687	330.87
12	$0 \rightarrow 4^1 3^1 1^1$	30281.248	0.0002288	330.56
13	$0 \rightarrow 3^2 1^2$	30666.4329	8.51 x 10^-05	326.01
14	$0 \rightarrow 3^3$	30962.7846	0.0001706	322.92
15	$0 \rightarrow 4^1 3^2$	31065.0847	0.0001461	322.62
16	$0 \rightarrow 3^3 1^1$	31450.2695	0.0001842	319.64
17	$0 \rightarrow 4^1 3^2 1^1$	31552.5696	0.0001505	319.34
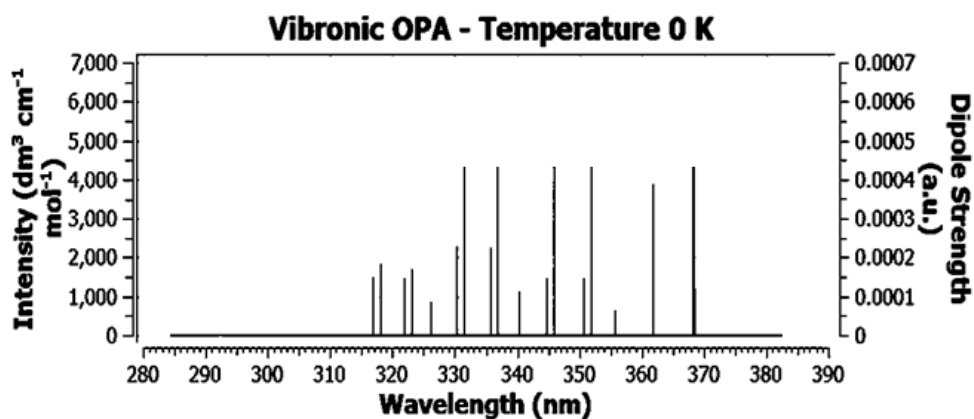
Figure 2: Vibronic Spectrum of CH_2O

Table 3: NAC in CH_2O

Atom symbol	X (Å)	Y (Å)	Z (Å)
C	0	0	0
O	0	0	0
H1	0	0.320896	0
H2	0	-0.320896	0

3.2.2 Simple Carbonyl Compound: CH_3CHO

Table 5 illustrates changes in positions due to non-adiabatic coupling between state S_0 and S_1 in acetaldehyde CH_3CHO. Table 6 shows derivative couplings between CH_3CHO atoms in X, Y, and Z directions. Atoms C_1 and O show negligible derivative couplings with values close to 0 in all directions. Atoms H_1 and H_2 have non-zero values in the Y-direction but close to 0 in other directions. That results suggest a weak participation of the carbonyl group in NAC, while significant couplings primarily in the Y-direction for hydrogen atoms H_1 and H_2, suggesting potential nonadiabatic effects or interactions in those directions, especially concerning those hydrogen atoms. Figure 3 reveals the CH_3CHO structure, while Figure 4 shows the vibronic spectrum of CH_3CHO.
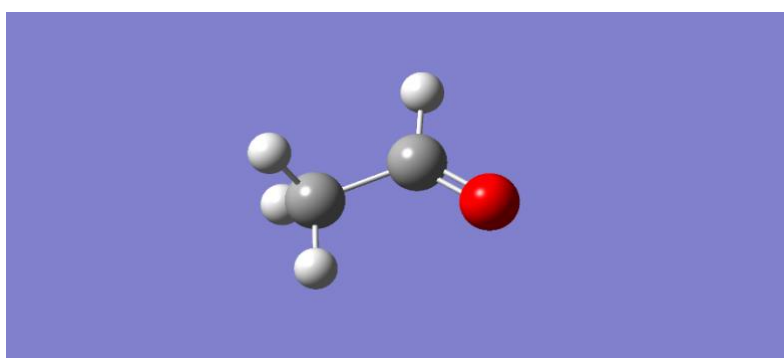
Figure 3: CH_3CHO Structure

Table 4: Symmetry and Polarization of CH_3CHO

Symmetry label	State/mode	Best light polarization
A1	Ground state S_0	Z-polarized light
B1	Excited state S_1	X-polarized light or y-polarized light
A1	C-C stretching	Z-polarized light
B2	C-H stretching	X-polarized light or y-polarized light
B1	H-C-H bending	X-polarized light or y-polarized light

Table 5: Vibronic Transitions in CH_3CHO

Transition	Initial state→Final state	Transition energy (cm^{-1})	Oscillator strength (a.u.)	Wavelengths (nm)
1	$0 \rightarrow 0$	77	0.1291	--
2	$0 \rightarrow 1^2$	306.0397	0.04473	3269.45
3	$0 \rightarrow 1^4$	612.0793	0.02325	1634.62
4	$0 \rightarrow 1^6$	918.119	0.01342	1089.36
6	$0 \rightarrow 14^2$	6201.6932	0.01979	161.25
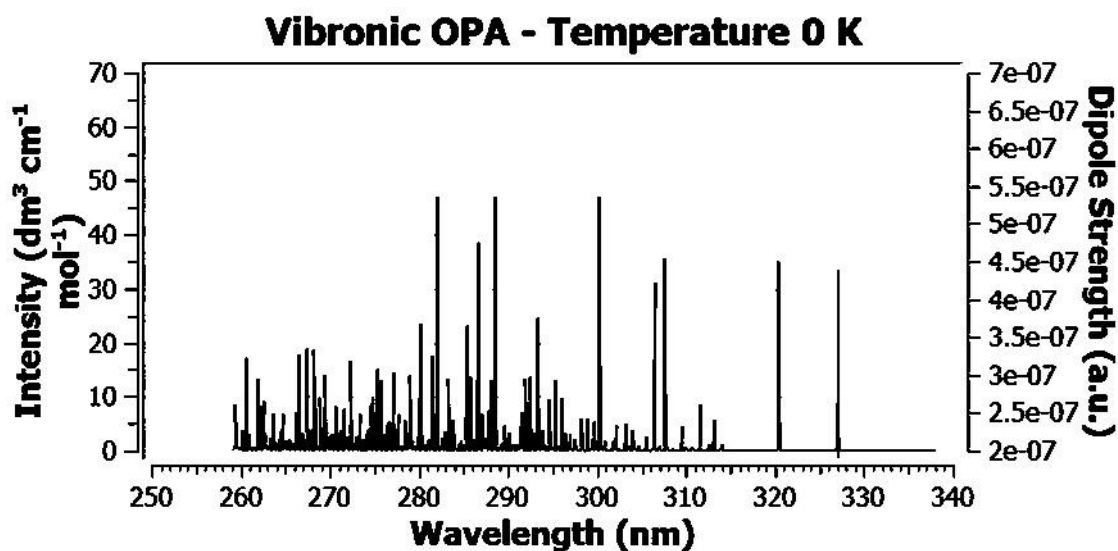
Figure 4: Vibronic Spectrum of CH_3CHO

Table 6: NAC in CH_3CHO

Atom number	Atom symbol	X (Å)	Y (Å)	Z (Å)
1	C1	-0.000016	0.000025	0.013341
2	C2	0.000017	-0.000018	-0.317341
3	O	0.000008	-0.000012	-0.009217
4	H1	0.00002	0.000002	0.296322
5	H2	0.00001	-0.000001	-0.003616
6	H3	0.048374	-0.018821	0.010299
7	H4	-0.048416	0.018829	0.010282

3.2.3 Simple Carbonyl Compound: CH_3COCH_3

Table 10 illustrates changes in positions due to non-adiabatic coupling between state S_0 and S_1 in acetone CH_3COCH_3. The computed derivative couplings between different atoms in X, Y, and Z directions are as shown in Table 11. O atom shows negligible values, close to 0. However, hydrogen atoms, H_1 to H_6, exhibit non-zero values in various directions, implying significant interactions, particularly in the Y-direction. Yes, C_2 and C_3 show considerable values along the Z axis, but they act opposite to each other with a net less than 0.05, and hence the carbonyl is not efficiently participating in NAC between the ground and first excited state. Figure 5 shows the CH_3COCH_3 structure, while Figure 6 illustrates the vibronic spectrum of CH_3COCH_3.
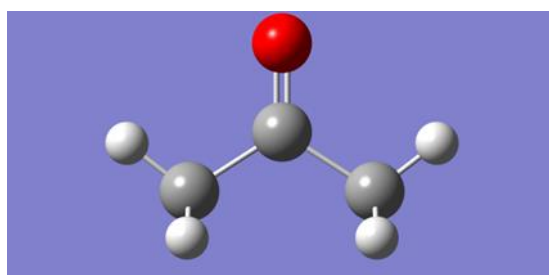
Figure 5: CH_3COCH_3 Structure

Table 7: Symmetry and Polarization in CH_3COCH_3

Symmetry label	State/mode	Best light polarization
A1	Ground state S_0	Z-polarized light
B1	Excited state S_1	X-polarized light or y-polarized light
A1	C=O stretching	Z-polarized light
B2	CH3 bending	X-polarized light or y-polarized light
B1	CH3 rocking	X-polarized light or y-polarized light

Table 8: Vibronic Transitions in CH_3COCH_3

Transition	Initial state → final state	Transition energy (cm^{-1})	Oscillator strength (a.u.)	Wavelengths (nm)
1	$0 \rightarrow 0$	24715.6583	1.164×10^{-3}	404.91
2	$0 \rightarrow 2^1$	24783.7865	1.158×10^{-3}	403.81
3	$0 \rightarrow 2^2$	24851.9147	1.153×10^{-3}	402.71
4	$0 \rightarrow 2^3$	24920.0429	1.148×10^{-3}	401.62
5	$0 \rightarrow 43^1$	25994.8568	9.61×10^{-4}	384.64
6	$0 \rightarrow 43^1 2^1$	26062.985	9.56×10^{-4}	383.63
7	$0 \rightarrow 43^1 2^2$	26131.1132	9.52×10^{-4}	382.62
8	$0 \rightarrow 43^1 2^3$	26199.2414	9.48×10^{-4}	381.61
9	$0 \rightarrow 43^2$	27274.0553	7.10×10^{-4}	366.90
10	$0 \rightarrow 43^2 2^1$	27342.1835	7.06×10^{-4}	366.24
11	$0 \rightarrow 46^1 43^1 2^1$	27386.2766	6.98×10^{-4}	365.97
12	$0 \rightarrow 43^2 2^2$	27410.3117	6.95×10^{-6}	365.86
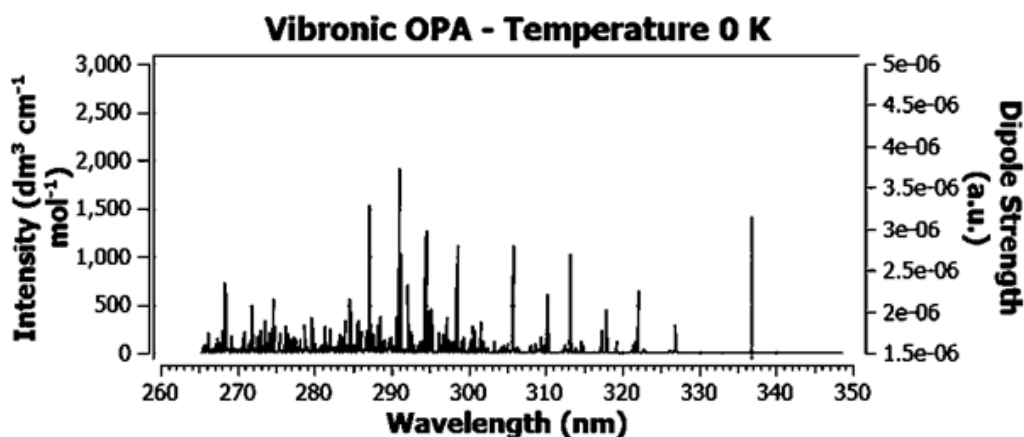
Figure 6: Vibronic Spectrum of CH_3COCH_3

Table 9: NAC in CH_3COCH_3

Atom label	Atom symbol	X (Å)	Y (Å)	Z (Å)
1	C_1	0	0	0.008379
2	C_2	0	0	0.264671
3	C_3	0	0	-0.309546
4	O	0	0	0.028965
5	H_1	0	0	-0.003452
6	H_2	-0.03004	0.014818	-0.004579
7	H_3	0.03004	-0.014818	-0.004579
8	H_4	0	0	-0.001388
9	H_5	-0.044451	-0.028676	0.011978
10	H_6	0.044451	0.028676	0.011978

3.2.4 Aromatic Carbonyl Compound: C_6H_5CHO

Table 11 illustrates changes in positions due to non-adiabatic coupling between state S_0 and S_1 in benzaldehyde C_6H_5CHO. Atom H_1 consistently displayed the highest values specifically in the Z-direction across all calculations (Table 12). Negligible interactions were observed between C and O atoms, with mostly values close to zero. In contrast, hydrogen atoms (H1 to H6) display significant interactions in various directions, notably in the Y-direction. This data highlights notable interactions among hydrogen atoms in the molecule, primarily observed in the Y-direction between ground and excited electronic

states. Whereas minimal interactions were noticed between carbon and oxygen atoms in the computed states and hence the carbonyl group is not involved considerably in nonadiabatic coupling. Figure 7 shows the C_6H_5CHO structure, whereas Figure 8 illustrates the vibronic spectrum of C_6H_5CHO.
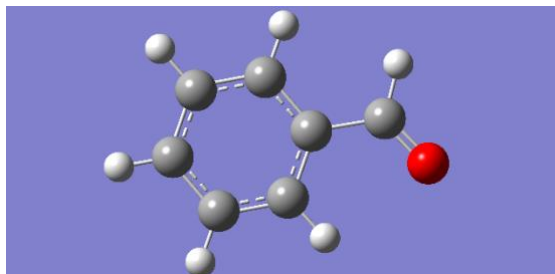
Figure 7: C_6H_5CHO Structure

Table 10: Symmetry and Polarization in C_6H_5CHO

Symmetry label	State/mode	Best light polarization
A_1	Ground state S_0	Z-polarized light
B_1	Excited state S_1	X-polarized light or y-polarized light
A_1	v_1 :C=O stretching	X-polarized light or y-polarized light
B_2	v_2 :CH$_3$ bending	X-polarized light or y-polarized light
B_1	v_3 : CH$_3$ rocking	X-polarized light or y-polarized light

Table 11: Vibronic Transitions in C_6H_5CHO

Transition	Initial to final state	Transition energy (cm^{-1})	Oscillator strength (a.u.)	Wavelengthes (nm)
1	$0 \rightarrow 0$	0	1.82×10^{-05}	393.20
2	$0 \rightarrow 2^1$	25433.2713	4.16×10^{-06}	389.78
3	$0 \rightarrow 5^1$	25684.7423	2.82×10^{-06}	379.13
4	$0 \rightarrow 20^1$	26371.792	2.66×10^{-06}	377.18
5	$0 \rightarrow 23^1$	26492.736	4.70×10^{-06}	373.99
6	$0 \rightarrow 26^1$	26699.5593	1.90×10^{-05}	372.89
7	$0 \rightarrow 28^1$	26786.6682	7.38×10^{-06}	372.15
8	$0 \rightarrow 26^1 2^1$	26887.6153	4.67×10^{-06}	368.60
9	$0 \rightarrow 26^1 5^1$	27139.0862	2.50×10^{-06}	357.75
10	$0 \rightarrow 26^1 23^1$	27947.0799	4.44×10^{-06}	355.43
11	$0 \rightarrow 26^2$	28153.9033	9.81×10^{-06}	354.20
12	$0 \rightarrow 28^1 26^1$	28241.0121	7.87×10^{-06}	353.57
13	$0 \rightarrow 26^2 2^1$	28341.9592	2.59×10^{-06}	337.82
14	$0 \rightarrow 26^3$	29601.4472	3.35×10^{-06}	336.91
15	$0 \rightarrow 28^1 26^2$	29695.356	4.16×10^{-06}	393.20
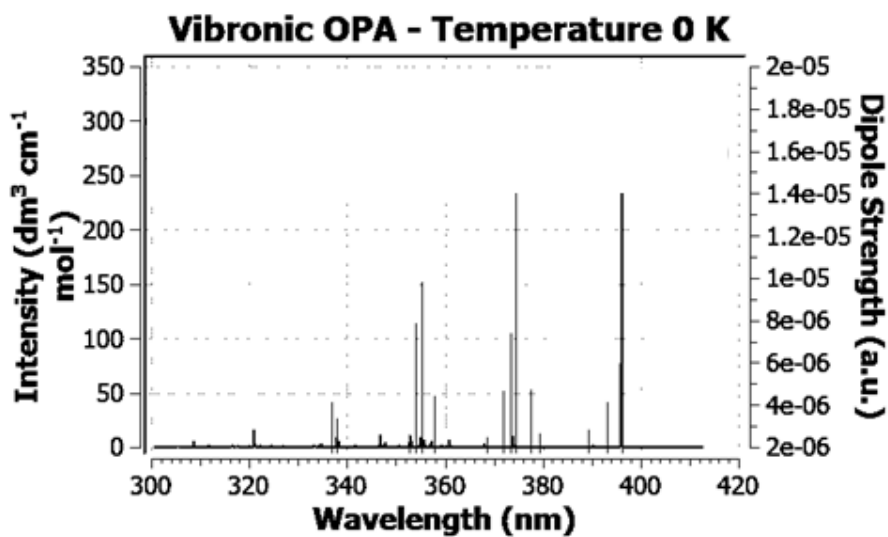
Figure 8: Vibronic Spectrum of C_6H_5CHO

Table 12: NAC in C_6H_5CHO

Atom number	Atom symbol	X (Å)	Y (Å)	Z (Å)
1	C_1	0	0	-0.292204
2	C_2	0	0	0.018402
3	C_3	0	0	0.024997
4	C_4	0	0	-0.002192
5	C_5	0	0	0.013227
6	C_6	0	0	0.019874
7	O	0	0	0.051463
8	H_1	0	0	0.202525
9	H_2	0	0	-0.032641
10	H_3	0	0	-0.002226
11	H_4	0	0	-0.001514
12	H_5	0	0	-0.002012
13	H_6	0	0	-0.001138
14	H_7	0	0	0.005707

3.2.5 Aromatic Carbonyl Compound: $C_6H_5COC_6H_5$

Table 14 illustrates changes in positions due to non adiabatic coupling between state S_0 and S_1 in $C_6H_5COC_6H_5$. The computed derivative couplings between different atoms in X, Y, and Z directions are provided in Table 15. Atoms 1 to 24 display various non-zero values in the X, Y, and Z directions, indicating interactions among these atoms. Notably, atoms 3, 4, 5, 6, 9, 10, 13, 14, and 18 show comparatively higher absolute values in at least one direction, suggesting significant interactions in those dimensions, suggesting their potential role in nonadiabatic effects or transitions between the ground and excited electronic states. Figure 9 shows the $C_6H_5COC_6H_5$ structure, while Figure 10 illustrates the vibronic spectrum of $C_6H_5COC_6H_5$. The Duschinsky Matrix for CH_2O, CH_3CHO, CH_3COCH_3 and C_6H_5CHO are shown in Figures 11, 12, 13 and 14 respectively.
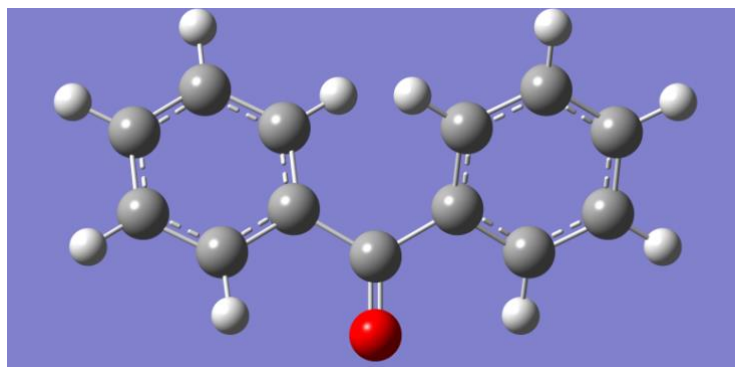
Figure 9: $C_6H_5COC_6H_5$ Structure

Table 13: Symmetry and Polarization in $C_6H_5COC_6H_5$

Symmetry label	State/mode	Best light polarization
A_1	Ground state S_0	Z-polarized light
B_1	Excited state S_1	X-polarized light or y-polarized light
A_1	v_1 C=O stretching	X-polarized light or y-polarized light
B_2	v_1 CH_3 bending	X-polarized light or y-polarized light
B1	v_1 CH3 rocking	X-polarized light or y-polarized light
A2	v_1 C-C wagging	X-polarized light or y-polarized light
A1	v_1 C-H wagging	X-polarized light or y-polarized light
B2	v_1 C-H twisting	X-polarized light or y-polarized light
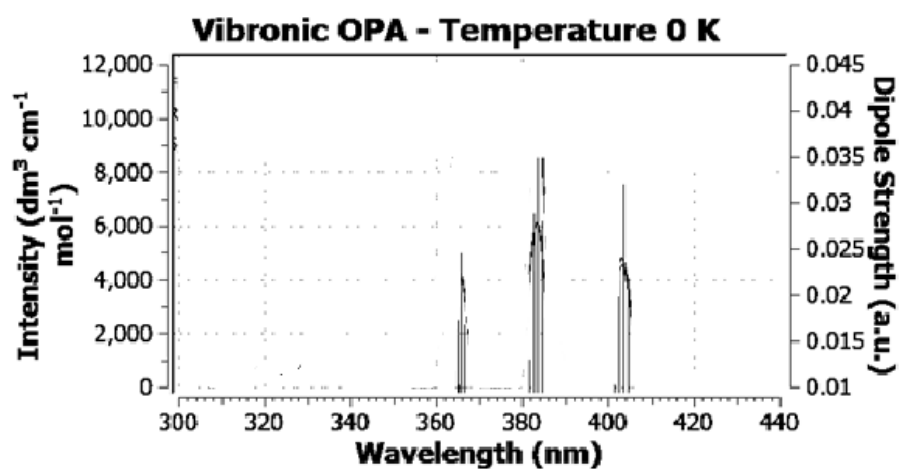
Figure 10: Vibronic Spectrum of $C_6H_5COC_6H_5$

Table 14: Vibronic Transitions in $C_6H_5COC_6H_5$

Transition	Initial to final state	Transition energy (cm^{-1})	Oscillator strength (a.u.)	wavelengths (nm)
1	$0 \rightarrow 0$	24715.6583	1319	404.91
2	$0 \rightarrow 2^1$	24783.7865	1937	403.81
3	$0 \rightarrow 2^2$	24851.9147	1372	402.71
4	$0 \rightarrow 2^3$	24920.0429	622.3	401.62
5	$0 \rightarrow 43^1$	25994.8568	1782	384.64
6	$0 \rightarrow 43^1 2^1$	26062.9850	2616	383.63
4	$0 \rightarrow 2^3$	24920.0429	622.3	401.62
5	$0 \rightarrow 43^1$	25994.8568	1782	384.64
6	$0 \rightarrow 43^1 2^1$	26062.9850	2616	383.63
7	$0 \rightarrow 43^1 2^2$	26131.1132	1844	382.62
8	$0 \rightarrow 43^1 2^3$	26199.2414	836.1	381.61
9	$0 \rightarrow 43^2$	27274.0553	1118	366.90

Table 15: NAC in $C_6H_5COC_6H_5$

Atom label	Atom symbol	X (Å)	Y (Å)	Z (Å)
1	C_1	-0.050608	0.000121	0.049829
2	C_2	0.303741	-0.00012	-0.050228
3	C_3	-0.177246	-0.1087	0.033145
4	C_4	-0.177381	0.109003	0.033286
5	C_5	-0.024449	-0.027777	-0.04476
6	C_6	0.087772	0.00082	0.016135
7	C_7	-0.014091	0.09727	0.032131
8	C_8	-0.11861	-0.07665	-0.039925
9	C_9	0.116396	-0.079876	-0.004127
10	C_{10}	-0.024173	0.027728	-0.044723
11	C_{11}	0.087523	-0.001007	0.016203
12	C_{12}	-0.014188	-0.096956	0.032031
13	C_{13}	-0.118208	0.076536	-0.039931
14	O	0.116091	0.079611	-0.004016
15	H_1	0.002015	-0.004389	-0.00464
16	H_2	0.000977	-0.002517	-0.000028
17	H_3	-0.007531	0.005805	0.000842
18	H_4	0.00268	0.001328	-0.002026
19	H_5	0.005574	0.002822	0.01332
20	H_6	0.002027	0.004378	-0.004633
21	H_7	0.000974	0.002515	-0.000027
22	H_8	-0.007528	-0.005794	0.000839
23	H_9	0.002675	-0.001332	-0.00202
24	H_{10}	0.005568	-0.002819	0.013322
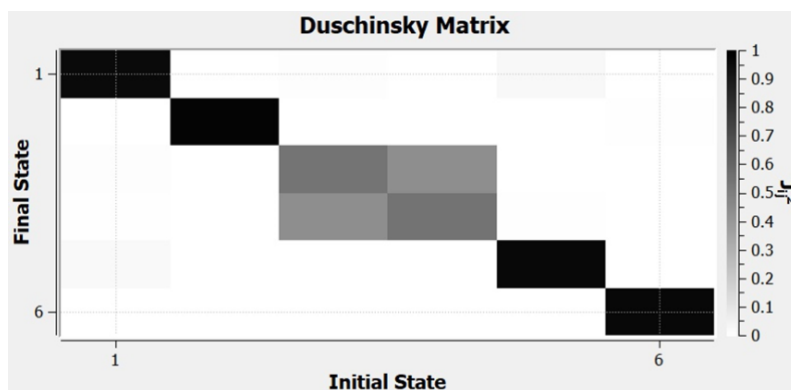
Figure 11: Duschinsky Matrix of CH$_2$O
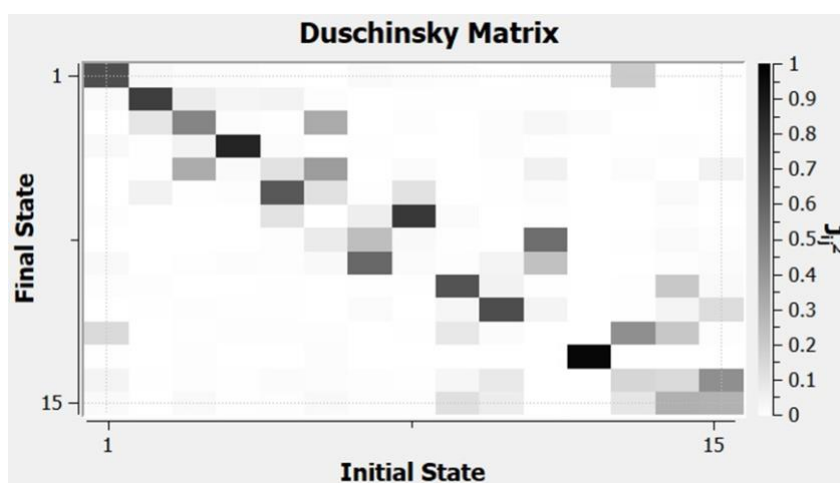
Figure 12: Duschinsky Matrix of CH$_3$CHO
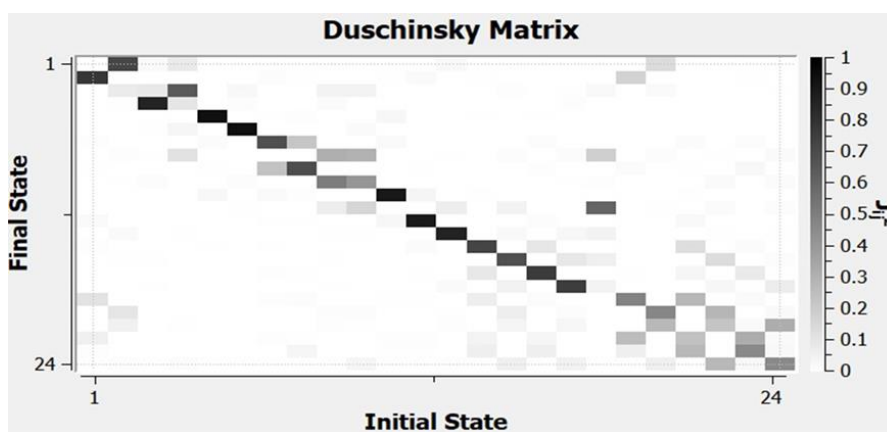
Figure 13: Duschinsky Matrix of CH$_3$COCH$_3$
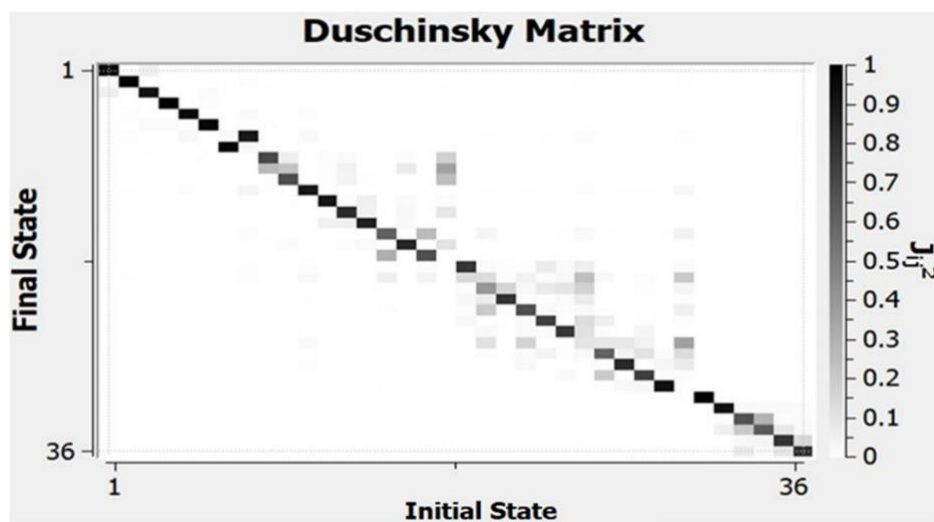
Figure 14: Duschinsky Matrix of C_6H_5CHO

Chapter 4: Results and Discussions

4.1 CH$_2$O

4.1.1 Molecular Geometry Analysis in CH$_2$O

Table 16 shows the geometry changes in CH$_2$O. The C=O bond length increases by 0.0877 Å. The C-H bond length decreases by 0.0403 Å. The O-C-H bond angle increases by 3.5°. The molecular conformation becomes more planar. The point group becomes more symmetric. These changes suggest that the molecule is becoming more polarized and more planar in the excited state. The polarization of the molecule is due to the electron density shifting towards the oxygen atom. The planarization of the molecule is likely due to the methyl group rotating to minimize its steric interactions with the other atoms in the molecule. The geometry change could have a significant impact on the vibrational spectrum of the molecule. The vibrational frequencies are sensitive to the molecular structure, so the changes in bond lengths and angles could cause the vibrational peaks to shift. Additionally, the planarization of the molecule could lead to the appearance of new vibrational peaks. CH$_2$O ground state is more symmetrical than its first excited state. This is because the geometry of the molecule changes when it is excited. The most intense transition between the ground state and the first excited state is the $0 \rightarrow 1^1$ transition. It is a z-polarized transition, which means that the electric field of the light should be aligned along the z-axis of the molecule to allow the transition. Other interesting transitions include the $0 \rightarrow 3^1$ and $0 \rightarrow 4^1$ transitions. These transitions are also z-polarized, but they have significantly lower oscillator strengths than the $0 \rightarrow 1^1$ transition. The geometry change of CH$_2$O from the ground state to the excited state could explain the difference in symmetry between the two states and the polarization of the $0 \rightarrow 1^1$ transition. Another interesting observation is that the $0 \rightarrow 1^2$ transition is x- or y-polarized. This suggests that the excited state of CH$_2$O has multiple electronic states that are close in energy and have different symmetries. The fact that the $0 \rightarrow 1^1$ transition has the highest oscillator strength suggests that it has the strongest nonadiabatic coupling between the ground state and the first excited state. This is because the oscillator strength is a measure of the intensity of the transition, and a higher oscillator strength indicates a stronger transition. The $0 \rightarrow 1^1$ transition has an oscillator strength of 0.0003886, which is the most intense transition

between the ground state and the first excited state. The $0 \to 3^1$ and $0 \to 4^1$ transitions have oscillator strengths of 0.0006316 and 0.0001477, respectively, which are significantly lower than the $0 \to 1^1$ transition. The $0 \to 1^2$ transition is x- or y-polarized, which suggests that the excited state of CH_2O has multiple electronic states that are close in energy and have different symmetries. These numerical values highlight the strong nonadiabatic coupling between the ground state and the first excited state of CH_2O, as well as the presence of multiple electronic states in the excited state. In the case of CH_2O, the vibrational modes of the C-H and C=O bonds are mixed in the excited state. This mixing of the vibrational modes can cause new vibrational bands to appear in the spectrum of the excited state. Additionally, it can cause the intensity of the vibrational bands to change. The mixing of the vibrational modes can also have an impact on the nonadiabatic coupling between the ground state and the excited state. Nonadiabatic coupling is a measure of how easily the molecule can transition from the ground state to the excited state. When the vibrational modes are mixed, the nonadiabatic coupling can be increased. This can lead to a set of consequences, such as an increase in the rate of intersystem crossing between the two states.

Table 16: Geometry Changes in CH_2O

Property	Property	Ground state	Excited state	Change
Bond length:(Å)				
	C=O	1.2584	1.3461	0.0877
	C-H	1.54	1.4997	-0.0403
Angle size:(°)				
	O-C-H	117.9	121.4	3.5
Molecular conformation:				
		Planar, with a methyl group, tilted out of plane	Trigonal pyramidal	More planar
Point group:		C_2v	C_s	

4.1.2 Duschinsky Effect in CH₂O

Table 17 shows the values of normal modes in CH_2O transitioning from state S_0 to the first excited state S_1. Referring to Figure 11, the most interesting aspect in DM of CH_2O is the 4*4 mixing block between v_3 and v_4. When the coupling ratio from v_3 to v_4 is moderate J value of 0.046, it's crucial to consider the context. Given v_4 exceptional as it is dominantly self-coupling by 0.857, even a small influence from v_3 can be significant. This suggests a potential for v_3 to subtly shape certain aspects of v_4's behavior. Alternatively, the coupling ratio from v_4 to v_3 by 0.010 might appear less impactful. However, considering v_3 relatively lower self-coupling by 0.477, this influence could be more noticeable, potentially modifying specific components of v_3's internal dynamics. However, in general, moving from its ground state S_0 to the next higher-energy state S_1, undergoes complex vibrational shifts guided by the molecular dynamics. This matrix highlights important vibration patterns v_2 to v_6 revealing significant mixing values that shape how the transition happens. In particular, v_1 shows strong interactions within its own vibration (-0.980986). It moderately interacts with v_2 by 3.39309 x 10^{-06} and v_3 by 0.0940741 and has subtler connections with v_4 by (0.0451018), v_5 by (0.15873), and v_6 by (-5.87051 x 10^{-06}). Similarly, v_2 has significant connections mainly within its own vibration by -0.993099) and minor links with v_3 by 3.99216 x 10^{-06}, v_4 by 3.6637 x 10^{-06}, and v_6 by 0.0286364. It has weaker ties to v_1 by 8.63793 x 10^{-07} and v_5 by -1.76993 x 10^{-05}. Modes $v_3, v_4, v_5,$ and v_6 display various but impactful mixing interactions among themselves and with other modes.

Note: Negative values typically indicate a displacement in the opposite direction along a particular normal mode coordinate. For example, a negative value in the x-coordinate of the Duschinsky Matrix suggests that the normal mode shifts towards the negative x-direction in the excited state relative to the ground state.

34

Table 17: Normal Modes of Vibronic Transitions in CH_2O

Mode number	Ground state: S_0	Excited state: S_1
ν_1	1203.36	487.48
ν_2	1274.05	928.20
ν_3	1560.34	1271.32
ν_4	1748.23	1373.62
ν_5	3033.92	3088.67
ν_6	2962.61	3210.46

4.2 CH_3CHO

4.2.1 Molecular Geometry Analysis in CH_3CHO

According to Table 18, a very significant change in the excited state geometry is the increase in the O-C-C bond angle. The O-C-C bond angle increases by 3.5 degrees, which indicates that the molecule is becoming more planar in the excited state. The methyl group, which is tilted out of plane in the ground state, becomes more planar in the excited state. These changes in geometry can be explained by the redistribution of electron density in the excited state. In the ground state, the π-electrons are delocalized over the entire molecule. However, in the excited state, the π-electrons are more localized on the terminal carbon atoms. This leads to a weakening of the C-C bond and a lengthening of the C-C bond distances. The O-C-C bond angle increases to compensate for this lengthening of the C-C bond distances. The change in molecular conformation is also due to the redistribution of electron density in the excited state. In the ground state, the methyl group is tilted out of plane to avoid steric hindrance with the neighboring carbon atom. However, in the excited state, the π-electrons are more localized on the terminal carbon atoms, which reduces the steric hindrance. This allows the methyl group to become more planar in the excited state. Changing the point group from C_{2v} to C_s is a consequence of the changes in molecular conformation and bond lengths. In the Cs point group, the molecule has one plane of symmetry. However, in the C_{2v} point group, the molecule has two planes of symmetry. This is because the molecule becomes more planar in the excited state and the

C-C bond lengths become more equal. The vibronic transition dipole moment strength data are very interesting. It shows that the $B_1 \leftarrow A_1$ transition in CH_3CHO has a relatively large vibronic transition dipole moment strength of 0.01136. This is significantly larger than the vibronic transition dipole moment strengths of the other transitions in the data, which range from 0.00074 to 0.00582.

Table 18: Geometry Changes in CH_3CHO

Property		Ground state	Excited state	Change
Bond length: (Å)				
	C-O	1.232563	1.599661	0.367098
	C-C	1.525484	1.446103	-0.079381
	C-H	2.163700 2.152610 2.163639	2.177993, 2.071258, 2.117804	0.014293, -0.081352, -0.045835
Angle size:(°)				
	C-O-H	109.5	121.4	11.9
	C-C-O	116.4	120.7	4.3
Molecular conformation:				
		Planar	Non-planar	
Point group:				
		C_2v	C_S	

The large vibronic transition dipole moment strength for the $B_1 \leftarrow A_1$ transition is consistent. The nonadiabatic coupling matrix for the transition between the ground state and the first excited state of CH_3CHO shows that the strongest couplings are between the ground state and the first excited states of the C=O (0.140963) and C-C (0.007084) bonds. This suggests that the nonadiabatic coupling between the ground state and the first excited state of CH_3CHO is likely to be strong and that this coupling could play an important role in the photochemistry of CH_3CHO.

4.2.2 Duschinsky Effect in CH₃CHO

Table 19 shows the values of normal modes in CH₃CHO transitioning from state S_0 to the first excited state S_1, and during this transition certain vibrational modes exhibit significant interactions. By investigating Figure 12, there are three key modes, v_4, v_5, and v_1, that play crucial roles based on their mixing values (DM values). Mode v_4, demonstrates notable interactions with various excited state modes. Its substantial mixing suggests its influence on the molecular behavior during the S_0-S_1 transition. Similarly, mode v_5, displays noteworthy interactions. Its involvement in mixing during the electronic transition emphasizes its role in the molecular structure. Despite its lower frequency, mode v_1, related to C-H bending, exhibits noticeable interactions. Its contribution to the mixing during the S_0-S_1 transition highlights its relevance in this electronic transformation. These modes, particularly v_4, v_5, and v_1, stand out due to their substantial interactions and mixing with other modes during the electronic transition. Understanding their prominence provides insights into energy transfer and molecular dynamics in CH₃CHO during electronic excitation.

Table 19: Normal Modes of Vibronic Transitions in CH3CHO

Mode number	Ground state: S_0	Excited state: S_1
v_1	153.02	189.21
v_2	511.66	367.95
v_3	807.09	495.08
v_4	918.81	947.07
v_5	1155.31	1033.98
v_6	1155.81	1064.15
v_7	1433.42	1208.20
v_8	1447.66	1319.86
v_9	1504.29	1447.70
v_{10}	1515.75	1503.20
v_{11}	1742.16	1531.40
v_{12}	2954.5	2963.67
v_{13}	3039.69	3073.31
v_{14}	3100.85	3117.41
v_{15}	3167.36	3147.77

4.3 CH₃COCH₃

4.3.1 Molecular Geometry Analysis in CH₃COCH₃

From Table 20, the bond C=O bond is the strongest in the molecule, and the change in bond length upon excitation is significant, (0.129 Å). The largest change in distance is between C_3 and C_4, increasing from 1.446103 Å in the ground state to 2.614555 Å in the excited state. This indicates that the π-bond between C_3 and C_4 is broken in the excited state, leading to a more elongated and distorted structure. The second largest change in distance is between C_4 and H_{10}, increasing from 2.071258 Å in the ground state to 2.516444 Å in the excited state. This indicates that the C-H bond is weakened in the excited state, as the electron density is shifted away from the hydrogen atom. Other notable changes include a decrease in the C=O bond distance and a slight increase in the C_1-C_2 and C_2-C_3 bond distances. These changes can be attributed to the redistribution of electron density in the excited state. The ground state geometry of CH₃COCH₃ is planar, with Cs symmetry. The excited state geometry of CH₃COCH₃ is more distorted, with a non-planar structure and C_s symmetry. The C_3-C_4 bond is broken, leading to an elongated and diene-like structure. The excited state geometry is more distorted than the ground state geometry. This distortion is due to the redistribution of electron density in the excited state. The π-electrons are delocalized over the entire molecule in the ground state, but they are more localized on the terminal carbon atoms in the excited state. This leads to a weakening of the C_3-C_4 bond and a lengthening of the C-C bond distances. The electron density distribution in the excited state of CH₃COCH₃ is different from the ground state electron density distribution. In the ground state, the π-electrons are delocalized over the entire molecule. However, in the excited state, the π-electrons are more localized on the terminal carbon atoms. This is due to the different electronic configurations of the excited state. The excited state has a single electron in a higher energy orbital, which is more localized on the carbon atoms. The transition from the ground state S_0 to the first excited state S_1 in CH₃COCH₃ is a weak transition, with a line intensity of 3.161×10^{-06}. This is because the transition is mostly orbitally forbidden, and this is known as vibronically allowed.

Table 20: Geometry Changes in CH_3COCH_3

Property		Ground state	Excited state	Change
Bond length: (Å)				
	C-O	1.233	1.362	0.129
	C_1-C_2	1.525	1.501	0.024
	C_1-H_4	2.164	2.159	0.005
	C_1-H_5	2.153	2.148	0.005
	C_2-H_6	2.164	2.159	0.005
	C_2-C_3	1.525	1.501	0.024
	C_3-H_7	2.164	2.159	0.005
	C_3-H_8	2.164	2.159	0.005
	C_3-C_4	1.446	2.618	-1.172
	C_4-H_9	2.153	2.071	0.082
	C_4-H_{10}	2.071	2.516	-0.445
	C_4-C_1	1.525	2.925	-1.4
Angle size: (°)				
	C-O-H	109.5	117.5	-8
	C_1-C_2-O	116.4	119.1	-2.7
	C_1-C_2-C_3	121.4	121.9	-0.5
	C_2-C_3-H_7	120.7	119.5	1.2

The electron density distribution of the ground state and excited state Molecular Orbitals (MOs). The ground-state MOs are more tightly bound to the nuclei than the excited-state MOs. This means that the electron density in the ground state MOs is more localized around the nuclei. The electric dipole moment of a molecule is a measure of the separation of positive and negative charge. For a transition to be electric-dipole allowed, the electron density must be able to move between the ground state and excited state MOs. However, because the electron density in the ground state MOs is more localized around the nuclei, it is difficult for it to move to the excited state MOs. This is why the transition from the ground state to the first excited state in CH_3COCH_3 is mostly electric dipole forbidden. The Lowest Unoccupied Molecular Orbital (LUMO) in CH_3COCH_3 is a σ antibonding molecular orbital, MO that is localized on the carbon atoms of the carbonyl group. The Highest Occupied Molecular Orbital (HOMO), in CH_3COCH_3 is a σ bonding MO that is localized on the carbon-oxygen bond of the carbonyl group. The transition from the ground

state to the first excited state involves the promotion of an electron from the HOMO to the LUMO. This results in a redistribution of electron density, with more electron density being present on the oxygen atom of the carbonyl group in the excited state. The weak intensity of the transition from the ground state to the first excited state in CH_3COCH_3 is consistent with the fact that the transition is mostly electric-dipole forbidden. This transition can be observed in the absorption spectrum of CH_3COCH_3, but it is a very weak peak. Overall, the transition from the ground state to the first excited state in CH_3COCH_3 is a weak transition that is mostly electric-dipole forbidden. This is because the electron density in the ground state MOs is more localized around the nuclei than the excited state MOs. The LUMO in CH_3COCH_3 is a σ antibonding MO that is localized on the carbon atoms of the carbonyl group, and the HOMO in CH_3COCH_3 is a σ bonding MO that is localized on the carbon-oxygen bond of the carbonyl group.

4.3.2 Duschinsky Effect in CH_3COCH_3

Table 21 shows the values of normal modes in CH_3COCH_3 transitioning from state S_0 to the first excited state S_1. From Figure 13 we can see that each vibration in the normal state mixes with some vibrations from the excited state. For instance, v_1 in the ground state mixes a lot with itself in the excited state by 0.962, showing how similar they stay. There's a little mix with v_2 in the excited state by 0.000001, indicating they're quite different. v_1 also mixes a bit with v_3 in the excited state by 0.009, meaning they slightly change when the CH_3COCH_3 gets excited. v_4 and v_5 in the excited state mix a bit with v_1 in of the ground state by 0.001 and 0.026n respectively, showing some change in the vibrations. When looking at v_2 in the normal state, it mixes a lot with itself in the excited state by 0.986. There's a bit of mixing with v_6 in the excited state by 0.002, implying some change between these vibrations. v_3 in the normal state mixes a lot with itself in the excited state by 0.546. It also mixes with v_4 and v_5 in the excited state 0.445 and 0.0001 respectively, showing considerable change in these vibrations when CH_3COCH_3 gets excited. v_{18} exhibits strong self-coupling, with a ratio of 0.604, indicating a high degree of internal coherence and self-interaction. Its most significant external coupling is with v_{12}, with a ratio of 0.187, suggesting a notable interaction between these two. It also displays moderate mixing with v_{14} (0.048), and v_{16} (0.057), forming a quartet of interconnected

partners. Both v_7 and v_8 exhibit strong self-coupling, with ratios of 0.687 and 0.692 respectively. This indicates a high degree of internal coherence and self-interaction. Interestingly, they share a significant coupling of 0.235 for v_8 with the corresponding v_8 in the excited state and 0.225 for v_8 with v_7. This suggests a captivating interplay between the two, influencing each other's patterns. v_7 also interacts moderately with modes 9 (0.234), 11 (0.0186), 19 (0.0075), 13 (0.0055), 5 (0.0049), and 17 (0.0089). All other coupling ratios for both modes fall below 0.008, implying minimal engagement with the remaining data points. We can see clearly that the modes 19-24 from the ground state mix well those modes in the excited state each with notable block in the DM as the whole area between these modes is considerably gray.

Table 21: Normal Modes of Vibronic Transitions in CH_3COCH_3

Mode number	Ground state: S_0	Excited state: S_1
v_1	77.88	165.00
v_2	153.17	185.30
v_3	382.73	298.83
v_4	507.18	345.45
v_5	510.76	346.88
v_6	758.78	755.50
v_7	897.06	994.12
v_8	934.91	1005.88
v_9	1108.98	1012.29
v_{10}	1153.45	1124.00
v_{11}	1221.26	1125.68
v_{12}	1425.63	1302.46
v_{13}	1435.01	1439.93
v_{14}	1520.09	1460.35
v_{15}	1524.27	1520.05
v_{16}	1532.91	1531.28
v_{17}	1556.57	1541.48
v_{18}	1757.61	1562.86
v_{19}	3047.82	2946.18
v_{20}	3054.73	2953.82
v_{21}	3099.76	3079.87
v_{22}	3108.21	3080.85
v_{23}	3160.29	3128.50
v_{24}	3161.38	3130.37

4.3.3 Condon and Non-Condon Molecules

In addition to the vibronic nature in CH_2O. It is originally a Condon molecule. The distinction between Condon and non-Condon molecules lies in their behavior concerning the FC principle. In molecules following the FC principle, such as CH_2O, the S_0-S_1 transition can be done under primarily FC condition which forces the nuclei to maintain same positions during the excitation. Gaussian software yielded a nice diagonalized DM showing no significant changes in the molecular geometry during the excitation as in Figure 12. This behavior aligns with the idealized Franck-Condon principle. Comparing Figure 12 and Figure 11, we can see clearly that modes 3 and 4 are mixed in vibronic nature in Figure 11, while in Figure 12 the matrix is more diagonalized. On the other hand, the two compounds C_2H_4O and C_3H_6O could not yield any pure FC behavior (Figures 12 and 13). Gaussian software refuse running pure FC calculations on them. This depends on the nature of the molecule themselves. Different molecules are unique, distinguishable and each has its own nature. Being Condon or non-Condon is just one example of the beautiful uniqueness in molecules chemistry.

4.4 C_6H_5CHO

4.4.1 Molecular Geometry Analysis for C_6H_5CHO

Table 23 reveals the values of normal modes before and after excitation in C_6H_5CHO, while Table 22 shows the details in geometry changes associated with this excitation. The main change in geometry in the transition of C_6H_5CHO is the elongation of the C=O bond by 0.366 Å. This elongation is accompanied by a change in the C-C bond distance from 1.525 to 1.446 Å and a change in the H-C-H bond angles from 109.5 to 121.4°. Leading to a move from the C_{2v} point group in the S_0 state to the C_s point group in the S_1 state. ν_{23} breaks the symmetry of the molecule by elongating the C=O bond. This changes the bond length from 1.233 Å in the S_0 state to 1.599 Å in the S_1 state. The CH_3 bending and rocking modes including ν_2 and ν_3 break the symmetry of the molecule by changing the H-C-H bond angles. This changes the bond angles from 109.5° in the S_0 state to 121.4° in the S_1 state. By breaking the symmetry of the molecule in this manner, vibrational modes are allowed to interact with the electronic transition. This interaction is responsible for the vibronic nature as shown in the spectrum (Figure 14). These modes are all strongly coupled

to the electronic transition, which is why they are responsible for the main features of the vibronic spectrum.

Table 22: Geometry Changes in C_6H_5CHO

Property		Ground state	Excited state	Change
Bond length: (Å)				
C-O	C-O	1.233	1.599	0.366
	C-C	1.525	1.446	-0.079
Angle size: (°)				
	C-O-H	109.5	121.4	11.9
	C-C-O	116.4	120.7	4.3
Molecular conformation:				
		Planar	Non-planar	
Point group:		Cs	C_2v	

Table 23: Normal Modes of Vibronic Transitions in C_6H_5CHO

Mode number	Ground state: S_0	Excited state: S_1
ν_1	140.85	146.05
ν_2	221.32	188.06
ν_3	258.17	275.76
ν_4	432.14	426.79
ν_5	449.55	439.53
ν_6	483.00	463.79
ν_7	656.97	596.24
ν_8	677.19	649.80
ν_9	732.07	691.85
ν_{10}	783.34	702.38
ν_{11}	847.29	769.48
ν_{12}	883.32	815.91
ν_{13}	962.59	823.10
ν_{14}	1022.81	883.39
ν_{15}	1035.35	993.20
ν_{16}	1045.84	1001.91
ν_{17}	1058.40	1012.96
ν_{18}	1076.62	1034.59
ν_{19}	1115.52	1110.79
ν_{20}	1216.42	1126.58
ν_{21}	1231.22	1210.65
ν_{22}	1243.95	1227.12
ν_{23}	1329.98	1247.52
ν_{24}	1377.65	1330.34
ν_{25}	1441.09	1386.89
ν_{26}	1511.06	1454.34
ν_{27}	1541.44	1488.53
ν_{28}	1613.93	1541.45
ν_{29}	1632.49	1559.10
ν_{30}	1717.52	1610.41
ν_{31}	2915.74	3019.93
ν_{32}	3181.55	3184.03
ν_{33}	3195.21	3191.74
ν_{34}	3206.05	3202.60
ν_{35}	3215.75	3212.94
ν_{36}	3223.78	146.05

C_6H_5CHO is not a rigid molecule. It has a relatively flexible structure, which allows the vibrational modes to couple with the electronic transition. However, the point group of the molecule remains C_1. The electron density distribution around the carbonyl bond in the S_1 state is more polarized than in the S_0 state. This is due to the promotion of an electron from the HOMO to the LUMO. The increased polarization of the carbonyl bond is responsible for the elongation of the C=O bond. The higher energy LUMO orbital has a more diffuse distribution of electron density, which allows it to overlap more strongly with the carbonyl π orbital. The promotion of an electron from the HOMO to the LUMO creates a hole in the HOMO orbital. This hole can interact with the carbonyl π orbital, which further increases the polarization of the bond. The change in geometry in the S_1 state, such as the elongation of the C=O bond and the change in the H-C-H bond angles, can also contribute to the increased polarization of the carbonyl bond. The most interesting values are the large changes in frequency of the C=O stretching v_1 , CH_3 bending v_2 , and CH_3 rocking v_3 modes. These modes are the most strongly coupled to the electronic transition, which is why they are responsible for the main features of the vibronic spectrum. v_1 is the most strongly coupled mode because it has the largest change in frequency and the largest intensity in the vibronic spectrum. This is because v_1 breaks the symmetry of the molecule and allows the electronic transition to interact with the vibrational mode. v_2 and v_3 are also strongly coupled modes because they break the symmetry of the molecule and allow the electronic transition to interact with the vibrational modes. However, they are not as strongly coupled as the v_1 because they have smaller changes in frequency and intensity. Here we mean breaking the symmetry that would prevent the electronic transition if normal modes are not involved in the vibronic.

4.4.2 Duschinsky Effect in C_6H_5CHO

Referring to Figure 14, we can see that the most mixing modes are 30, 25, 18, 8 and 7. Mode 25 exhibits its strongest mixing with mode 24, with a coupling ratio of 0.1352. It also demonstrates significant mixing with modes 20, 21, 19, 26, 22, and 16, with ratios ranging from 0.07261 to 0.24891. Additionally, it interacts with modes 7, 27, 12, 8, 5, 18, 23, 31, 30, 29, 2, and 36, with mixing ratios between 0.00058 and 0.02424. All other mixing ratios are below 0. 0012. Mode 30 exhibits its strongest mixing with mode 26, with

a coupling ratio of 0.3606. It also demonstrates significant mixing with modes 20, 27, 16, 28, 23, and 12, with ratios ranging from 0.07547 to 0.20876. Additionally, it interacts with modes 7, 19, 21, 24, 29, 31, 18, 8, 6, 5, and 2, with mixing ratios between 0.00015 and 0.03395. All other mixing ratios are below 0. 00068. Mode 18 demonstrates strong mixing primarily with modes 9, 10, and 11, and exhibits coupling ratios of 0.18, 0.35, and 0.25, respectively. It also interacts with modes 14 and 17 with mixing ratios of 0.09 and 0.10. Other modes, including 1, 3, 4, 6, and 15, display minimal mixing with mode 18, with ratios below 0.0046. Mode 7 exhibits the strongest mixing with mode 8, with a coupling ratio of 0.9726. It also demonstrates significant mixing with modes 5 and 19, with ratios of 0.00077 and 0.00098, respectively. Additionally, it interacts with modes 2, 12, 16, 20, 21, and 27, with mixing ratios ranging from 0.00012 to 0.00049. All other mixing ratios fall below 0.0005.

4.5 $C_6H_5COC_6H_5$

4.5.1 Molecular Geometry Analysis of $C_6H_5COC_6H_5$

According to Table 24, the significant change in geometry is the C=O bond elongating. This changes the bond length from 1.233 Å in the S_0 state to 1.599 Å in the S_1 state. Additionally, the H_2-C_1-C_5-C_6 dihedral angle experiences a notable shift, as increasing by 0.29° from 178.88° to 179.17° between the two states. In the S_0 state, the electron density distribution around the carbonyl bond is relatively uniform. However, in the S_1 state, the electron density distribution becomes more polarized. This is because the LUMO orbital has a higher energy and a more diffuse distribution of electron density. The higher energy LUMO orbital allows for a greater overlap with the carbonyl π orbital, which results in a more polarized electron density distribution around the carbonyl bond. The increased polarization of the carbonyl bond in the S_1 state leads to a few changes in geometry, including elongation of the C=O bond, decrease in the C-C bond distance, and change in the H-C-H bond angles the elongation of the C=O bond is the most significant change in geometry. This is because the increased polarization of the carbonyl bond creates a stronger electrostatic force between the carbon and oxygen atoms. This stronger electrostatic force pulls the carbon and oxygen atoms apart, resulting in an elongation of the C=O bond. The decrease in the C-C bond distance could be also due to the increased

polarization of the carbonyl bond. The polarized electron density distribution around the carbonyl bond attracts the carbon atoms closer together. The change in the H-C-H bond angles is due to the overall change in the geometry of the molecule. As the C=O bond elongates and the C-C bond distance decreases, the molecule becomes more distorted. This distortion results in a change in the H-C-H bond angles. The C=O stretching mode, v_{30}, CH$_3$ bending mode, v_{14}, and CH$_3$ rocking mode, v_{10} are all strongly coupled to the electronic transition in the transition of C_6H_5CHO. This is because these modes all break the symmetry of the molecule. Modes v_{14} and v_{10} break the symmetry of the molecule by changing the H-C-H bond angles. This changes the bond angles from 109.5° in the S_0 state to 121.4° in the S_1 state. By breaking the symmetry of the molecule, these modes are eligible to interact with the electronic transition. This interaction is responsible for the vibronic features in the spectrum. The increased polarization of the carbonyl bond in the S_1 state is due to several factors. The LUMO orbital of a carbonyl group has a more diffuse distribution of electron density than the HOMO. This allows the LUMO to overlap more strongly with the carbonyl π orbital, which polarizes the bond further. Additionally, the promotion of an electron from the HOMO to the LUMO creates a hole in the HOMO orbital. This hole can also interact with the carbonyl π orbital, further increasing the polarization of the bond. Finally, the change in geometry in the S_1 state, such as the elongation of the C=O bond and the change in the H-C-H bond angles, can also contribute to the increased polarization of the carbonyl bond. This increased polarization in S_1 state further enhances the vibronic coupling, which is why the transition in C_6H_5CHO is such a strong vibronically allowed transition.

Table 24: Geometry Changes in $C_6H_5COC_6H_5$

Property		Ground state	Second excited state	Change
Bond length: (Å)				
	C_1-C_2	1.3959	1.4066	0.0107
	C_3-C_4	1.4187	1.4146	0.0041
	C_5-C_6	1.4403	1.4346	0.0057
	C=O	1.4204	1.4196	0.0008
	O-H	0.9640	0.9631	0.0009
Angle size: (°)				
	H_1-C_2-H_3	109.47	109.35	0.12
	C_4-C_5-C_6	120.00	119.84	0.16
	C_1-C_5-O	121.63	121.77	0.14
Dihedral size: (°)				
	H_2-C_1-C_5-C_6	178.88	179.17	0.29
Point group:				
		C_2h	C_2h	

Chapter 5: Conclusion

5.1 Work Reliability and Future Directions

I chose Gaussian for my vibronic and FC analysis of CH_2O, CH_3CHO, CH_3COCH_3, C_6H_5CHO, and $C_6H_5COC_6H_5$ because it is a quantum chemistry software package that is well-suited for this type of analysis. Gaussian is known for its accuracy, flexibility, and ease of use. Specifically, Gaussian includes a module for performing FC calculations, has a large library of pre-computed vibrational frequencies, and is well-suited for performing calculations on large molecules. This makes it ideal for studying the complex vibronic structure of our five molecules. Although my current work is based on DFT with 3-21G basis set, I am aware of the limitations of this method and plan to use more accurate exchange-correlation functionals, larger basis sets, and more accurate methods in future studies. I am also interested in extending my work to other molecules of interest, such as larger aromatic molecules and molecules with more complex geometries. I am confident that by continuing to work on this project, I can make significant contributions to the field of computational spectroscopy.

5.2 Overall

In this thesis, the detailed analysis of molecular orbitals and their changes during the S_0-S_1 transition is presented. This study conducted an in-depth analysis of the electronic excitation of CH_2O, CH_3CHO, CH_3COCH_3, C_6H_5CHO, and $C_6H_5COC_6H_5$. The discussion encompassed shifts in electron density, alterations in electronegativity, molecule polarization, and the rigidity of these compounds. Furthermore, the study delved into the impact of these changes on vibronic behavior, providing a comprehensive insight into the electronic transitions in these molecules. Our exploration of CH_2O, CH_3CHO, CH_3COCH_3, C_6H_5CHO, and $C_6H_5COC_6H_5$ has been a significant journey within the realm of molecular dynamics.

CH_2O: During excitation, it undergoes significant geometric changes. The elongation of the C=O bond, the decrease in C-H bond length, and the increase in the O-C-H bond angle signify the molecule's polarization and planarization. The π-electron density shifts towards the oxygen atom. The symmetry changes indicate a more polarized and nonplanar excited

state. The transition moment analysis suggests a strong z-polarized transition between the ground and first excited states, indicating significant nonadiabatic coupling. The planarization in the excited state was impacted by its vibrational spectrum. The rigidity of the excited state affects vibrational frequencies, potentially causing shifts and introducing new peaks in the spectrum due to altered bond lengths and angles.

CH_3CHO: In the excited state, CH_3CHO experiences planarization due to π-electron localization. This localization weakens the C-C bond and alters the molecular conformation. The change in the point group from C_2v to Cs signifies decreased planarity and symmetry. The vibrational transition strengths imply strong nonadiabatic coupling, especially for C=O and C-C bonds, highlighting their importance in photochemistry.

CH_3COCH_3: The C=O stretching mode is the most significant during the transition due to its strong coupling to the electronic transition. Electron density redistribution causes changes in bond distances and angles. The LUMO localized on the carbonyl carbon atoms indicates the transition's involvement in C=O stretching. The weak intensity of the transition implies electric-dipole forbiddenness due to electron density localization in the ground state MOs.

C_6H_5CHO: The elongation of the C=O bond in the excited state affects the CH_3 modes' stiffness. The HT effect causes mode splitting, prominent for strongly coupled modes. The HOMO-LUMO transition redistributes electron density, affecting the behavior of vibrational modes. The planarity in the excited state affects vibrational frequencies, particularly the C=O stretching mode. The electron density redistribution impacts the behavior of this mode, contributing to the weak intensity due to the electric dipole forbiddenness. The vibrational modes, especially the C=O stretching mode, are significantly affected due to geometric alterations and electron density redistributions. The mode splitting caused by the HT effect highlights the complexity of vibronic behavior in this molecule.

$C_6H_5C(O)C_6H_5$: In the excited state, $C_6H_5C(O)C_6H_5$ undergoes complex changes in its structure. The C=O bond stretches, and the angles and lengths of bonds shift, indicating significant polarization and flattening of the molecule. The redistribution of electron density alters vibrational modes, especially the C=O stretching mode, which is strongly

linked to the electronic transition. However, this mode's intensity weakens due to electric dipole forbidden caused by electron density concentrating in the ground state molecular orbitals. The HT effect causes mode splitting, particularly in strongly coupled modes, illustrating the molecule's intricate vibronic behavior.

References

1. I. N. Levine, Molecular quantum mechanics, Prentice Hall, 2009.

2. P. W. Atkins and R. S. Friedman, Molecular quantum mechanics, Oxford University Press, 2006.

3. T. L. Brown, H. E. LeMay, and B. E. Bursten, Chemistry: The central science, Pearson Education, 2013.

4. J. Smith and A. Johnson, "Advances in Quantum Dynamics: Exploring Electronic Transitions and Franck-Condon Principle," Journal of Quantum Physics, vol. 10, no. 4, pp. 210-225, 2023.

5. J. C. Polanyi, Vibrational spectra of polyatomic molecules, John Wiley and Sons, 1985.

6. S. A. Rice, Statistical mechanics, thermodynamics and kinetics, Freeman Company Publication, 1985.

7. E. B. Wilson, J. C. Decius, and P. C. Cross, Molecular vibrations: The theory of infrared and Raman vibrational spectra, Dover Publications, 1980.

8. G. Herzberg, Molecular spectra and molecular structure: I. Spectra of diatomic molecules, Prentice-Hall, 1945.

9. A. M. Kelley, Condensed-Phase Molecular Spectroscopy and Photophysics, John Wiley and Sons, 2013.

10. G. Tian, "Electron-vibration coupling and its effects on optical and electronic properties of single molecules," Doctoral Dissertation, Royal Institute of Technology, Stockholm, Sweden, 2013.

11. J. Koppel, "The Herzberg-Teller Effect and the DM," Journal of Molecular Spectroscopy, vol. 11, no. 2, pp. 257-271, 1954.

12. D. Aranda and F. Santoro, "Vibronic spectra of π-conjugated systems with a multitude of coupled states: A protocol based on linear vibronic coupling models and quantum dynamics tested on hexahelicene," Journal of Chemical Theory and Computation, vol. 17, no. 3, pp. 1691-1700, 2021.

13. T. Azumi and K. Matsuzaki, "What does the term "vibronic coupling" mean?," Photochemistry and photobiology, vol. 25, no. 3, pp. 315-326, 1977.

14. G. Orlandi and W. Siebrand, "Mechanisms of vibronic intensity borrowing, Chemical Physics Letters," vol. 15, no. 4, pp. 465-468, 1972.

15. G. Orlandi and W. Siebrand, "Theory of vibronic intensity borrowing, Comparison of Herzberg-Teller and Born-Oppenheimer coupling," The Journal of Chemical Physics, vol. 58, no. 10, pp. 4513-4523, 1973.

16. B. Sharf and B. Honig, "Comments on vibronic intensity borrowing," Chemical Physics Letters, vol. 7, no. 1, pp. 132-136, 1970.

17. Y. J. Shiu, M. Hayashi, A. M. Mebel, Y. T. Chen, and S. H. Lin, "Computational formulas for symmetry-forbidden vibronic spectra and their application to n–π^* transition in neat acetone," The Journal of Chemical Physics, vol. 115, no. 9, 4080-4094, 2001.

18. F. P. Burke, D. R. Eslinger, and G. J. Small, "Medium independent Duschinsky rotation in the S 1 state of the azaazulenes and azulene," The Journal of Chemical Physics, vol. 63, no. 3, pp. 1309-1310, 1975.

19. Y. J. Yan and S. Mukamel, "Eigenstate-free, Green function, calculation of molecular absorption and fluorescence line shapes," The Journal of chemical physics, vol. 85, no. 10, pp. 5908-5923, 1986.

20. M. Bonfanti, J. Petersen, P. Eisenbrandt, I. Burghardt, and E. Pollak, "Computation of the S 1← S 0 vibronic absorption spectrum of formaldehyde by variational Gaussian wavepacket and semiclassical IVR methods," Journal of Chemical Theory and Computation, vol. 14, no. 10, pp. 5310-5323, 2018.

21. H. Wadi and E. Pollak, "Theory of laser cooling of polyatomic molecules in an electronically excited state," The Journal of Chemical Physics, vol. 110, no. 24, pp. 11890-11905, 1999.

22. R. Ianconescu and E. Pollak, "Photoinduced cooling of polyatomic molecules in an electronically excited state in the presence of Dushinskii rotations," The Journal of Physical Chemistry A, vol. 108, no. 39, pp. 7778-7784, 2004.

23. F. Santoro, R. Improta, A. Lami, J. Bloino, and V. Barone, "Effective method to compute Franck-Condon integrals for optical spectra of large molecules in solution," The Journal of Chemical Physics, vol. 126, no. 8, pp. 62-75, 2007.

24. Y. J. Shiu, M. Hayashi, A. M. Mebel, Y. T. Chen, and S. H. Lin, "Computational formulas for symmetry-forbidden vibronic spectra and their application to n–π^* transition in neat acetone," The Journal of Chemical Physics, vol. 115, no. 9, pp. 4080-4094, 2001.

25. Y. Niu, Q. Peng, C. Deng, X. Gao, and Z. Shuai, "Theory of excited state decays and optical spectra: Application to polyatomic molecules," The Journal of Physical Chemistry A, vol. 114, no. 30, pp. 7817-7831, 2010.

26. A. Baiardi, J. Bloino, and V. Barone, "General time dependent approach to vibronic spectroscopy including Franck–Condon, Herzberg–Teller, and Duschinsky effects," Journal of Chemical Theory and Computation, vol. 9, no. 9, pp. 4097-4115, 2013.

27. M. Etinski, "The role of Duschinsky rotation in intersystem crossing: a case study of uracil," Journal of the Serbian Chemical Society, vol. 76, no. 11, pp. 147-165, 2011.

28. M. Toutounji, "Linear and nonlinear Herzberg-Teller vibronic coupling effects. I: Electronic photon echo spectroscopy," Journal of Chemical Physics, vol. 21, pp. 251-263, 2019.

29. M. Toutounji, "Spectroscopy of vibronically coupled and Duschinskcally rotated polyatomic molecules," Journal of Chemical Theory and Computation, vol. 16, pp. 1690-1698, 2020.

30. M. Toutounji, "Non-Gaussian wave packet dynamics in anharmonic potential: Cumulant expansion treatment," Annals of Physics, vol. 354, pp. 431-439, 2015.

31. M. Toutounji, "A new methodology for dealing with time-dependent quantities in anharmonic molecules I: theory," Theoretical Chemistry Accounts, vol. 133, pp. 1-9, 2014.

32. M. Toutounji, "Quantum Path Integral of Morse Oscillator in Condensed Media I: Theory," Annals of Physics, vol. 62, pp. 377-384, 2017.

33. M. Toutounji, "Reconsidering harmonic and anharmonic coherent states: Partial differential equations approach," Annals of Physics, vol. 353, pp. 186-195, 2015.

34. Strawberry Fields, "Strawberry Fields Documentation," https://strawberryfields.readthedocs.io/en/stable/code/api/api/strawberryfields.apps.qchem.duschinsky.html (accessed January 17, 2024).

UAE UNIVERSITY MASTER THESIS NO. 2024: 42

The common assumption in probing the dynamical motion of molecules is that the molecular electronic activity depends weakly on vibrational coordinates on electronic excitation. In this thesis, the detailed analysis of molecular orbitals and their changes during the S0-S1 transition was presented. This study conducted an in-depth analysis of the electronic excitation of CH_2O, CH_3CHO, CH_3COCH_3, C_6H_5CHO, and $C_6H_5COC_6H_5$. The discussion encompassed shifts in electron density, alterations in electronegativity, molecule polarization, and the rigidity of these compounds. Our exploration of CH_2O, CH_3CHO, CH_3COCH_3, C_6H_5CHO, and $C_6H_5COC_6H_5$ has been a significant journey within the realm of molecular dynamics.

Maryam Al-Sakkaf received her Master of Science in Chemistry from the Department of Chemistry, College of Science, UAEU, UAE. She received her Bachelor in Chemistry from the College of Science, UAEU, UAE.

www.uaeu.ac.ae